Lung Cancer (2008) 60, 125–131

available at www.sciencedirect.com

ScienceDirect

journal homepage: www.elsevier.com/locate/lungcan

lungcancer

SHORT COMMUNICATION

Mucoepidermoid carcinoma of the lung: High-resolution CT and histopathologic findings in five cases

Taichiro Ishizumi[a,b], Ukihide Tateishi[a], Shun-ichi Watanabe[b], Yoshihiro Matsuno[c]

[a] *Divisions of Diagnostic Radiology and Nuclear Medicine, National Cancer Center Hospital, 5-1-1, Tsukiji, Chuo-Ku, 104-0045 Tokyo, Japan*
[b] *Divisions of Thoracic Surgery, National Cancer Center Hospital, 5-1-1, Tsukiji, Chuo-Ku, 104-0045 Tokyo, Japan*
[c] *Divisions of Pathology, National Cancer Center Hospital, 5-1-1, Tsukiji, Chuo-Ku, 104-0045 Tokyo, Japan*

Received 13 December 2006; received in revised form 30 June 2007; accepted 21 August 2007

KEYWORDS
Mucoepidermoid carcinoma;
Lung;
High-resolution CT

Summary
Objective: The purpose of this study was to characterize the high-resolution computed tomography (HRCT) findings of mucoepidermoid carcinoma of the lung and correlate them with the histopathological features.
Methods: The study included five patients with pathologically proven mucoepidermoid carcinoma who underwent HRCT before treatment. The HRCT findings were then compared with the histopathological features in all patients.
Results: The HRCT images showed lesions in the central lung in four patients and in the peripheral lung in one. All the lesions were well defined nodules or masses with a smooth margin. The contour of the tumours was oval ($n=3$), round ($n=1$) or lobulated ($n=1$). The contrast-enhanced CT images showed marked heterogeneous enhancement with foci of relatively low attenuation in four of the five lesions and mild heterogeneous enhancement in the other lesion. There was an admixed distribution of areas that are heterogeneous in the densities of blood vessels, as highlighted by immunohistochemical staining of CD31. Most mucin-secreting areas of the tumours showed more densely distributed blood vessels, mostly capillaries, in between tumour cell nests, whereas other areas did less. All five patients in our series underwent lobectomy plus lymph node dissection or sampling. All the patients are alive without evidence of disease an average of 50.4 months after surgery (range, 15–82 months; median, 57 months).

Corresponding author at: Divisions of Diagnostic Radiology and Nuclear Medicine, National Cancer Center Hospital, 5-1-1, Tsukiji, Chuo-Ku, 104-0045 Tokyo, Japan. Tel.: +81 3 3542 2511; fax: +81 3 3542 3815.
E-mail address: tishizumi@hotmail.co.jp (T. Ishizumi).

0169-5002/$ – see front matter
doi:10.1016/j.lungcan.2007.08.022

Conclusion: Mucoepidermoid carcinoma of the bronchus is often visualized as marked heterogeneous contrast enhancement on HRCT images. The results of this study suggest that the presence of abundant microvessels, detected immunohistochemically by microscopic examination, affects the enhancement pattern on HRCT.

1. Introduction

Mucoepidermoid carcinoma of the lung is an extremely rare tumour, comprising less than 5% of primary bronchial tumours and 0.1–0.2% of all lung cancers [1–4]. The largest series (56 cases over 26 years) has been published by Yousem and Hochholzer [3]. These tumours are thought to originate from bronchial gland of minor salivary gland-type lining the bronchi, and are classified into low grade and high grade on the basis of histological criteria [1,3,5]. The most important factors in the prognosis include the histological grade and whether complete surgical resection is possible. Completely resectable low-grade tumours generally have an excellent prognosis [3,6].

The radiological appearance of mucoepidermoid carcinoma of the lung depends on tumour location, size and whether obstructive pneumonia is present. The reported computed tomographic (CT) appearance of mucoepidermoid carcinoma of the lung is a well circumscribed oval or lobulated mass arising within the bronchus [7]. Although some investigators have reported the CT features of this tumour [7–10], few reports have included detailed findings of high-resolution CT (HRCT) or correlated them with histopathologic features. The purpose of this study was to characterize the HRCT findings of mucoepidermoid carcinoma of the lung and correlate them with the histopathologic features.

2. Materials and methods

The patients investigated in this study presented at the National Cancer Center, Tokyo, Japan, for diagnosis and treatment during the period from January 1999 through December 2005. Only patients with primary mucoepidermoid carcinoma of the lung were included; patients with pulmonary metastasis from remote sites were excluded. Five patients underwent HRCT and were treated for primary mucoepidermoid carcinoma. The diagnosis was confirmed by histopathologic examination of the surgical specimen in all five patients. All clinical records, including the follow-up information, HRCT findings, endoscopic images and gross and microscopic specimens, were reviewed retrospectively.

2.1. HRCT protocols

HRCT was performed with either a 4-row or 16-row multi-detector CT (MDCT) scanner (Aquilion V-detector, Toshiba Medical Systems Corp., Tokyo Japan). The patients were evaluated with the MDCT scanner by using axial 2.0 mm × 4 mm or 16 modes, 120 kVp, 200–250 mA, and thin-section CT images were obtained using 1.0 mm sections reconstructed at 2.0 mm intervals with a high-spatial-frequency algorithm and retrospectively retargeted to each lung with a 20 cm field of view (FOV). All patients were intravenously injected with 80–150 ml of non-ionic contrast medium at a rate of 2.0–3.0 ml/s with an autoinjector (Autoenhance A-250, Nemoto Kyorindo, Tokyo, Japan), and scanning was started after a 40 s delay. Hard-copy images were photographed at window settings for the lung (center, −600 HU; width, 2000 HU) and the mediastinum (center, 35 HU; width, 400 HU). The intervals between the CT examinations and surgery ranged from 2 days to 4 weeks. All patients were followed up regularly in our institute. Follow-up CT images were obtained in all patients.

The HRCT images were assessed by two independent observers without reference to the clinical findings. The location of the pulmonary nodule was classified as peripheral or central. Nodules present within the peripheral two-thirds of the lung were arbitrarily classified as peripheral type and those within the central one-third or in contact with lobar or segmental bronchi were classified as central. The CT analysis included determination of the attenuation coefficient of the pulmonary lesion. CT attenuation coefficient was evaluated before and after administration of contrast media. The contrast enhancement of the tumour was compared with that of the chest wall musculature. Whether intratumoral calcification was present was also noted. After making independent initial evaluations, the two observers reviewed all cases in which their interpretations differed and reached a final consensus.

2.2. Histopathologic examination

Surgical specimens were inflated and fixed by transpleural and transbronchial infusion with formalin. The specimens were sectioned transversely in the same planes as the HRCT images, stained with hematoxylin-eosin and immunostained for the endothelial marker CD31. One of the authors, an experienced pulmonary pathologist, reviewed the histopathologic findings. The characteristics of the tumours on the HRCT images were compared with the histopathologic findings.

3. Results

3.1. Clinical features

The clinical data are summarized in Table 1. The five patients (two males and three females) ranged in age from 22 to 58 years, and their average age was 41.6 years. Only two of them were smokers. Four of the patients complained of chronic symptoms, including cough, increased sputum production and episodic fevers. These symptoms were related to bronchial irritation, partial or complete bronchial obstruction and distal pneumonia. The remain-

Table 1 Clinical data of patients with mucoepidermoid carcinoma of the bronchus

Case	Age (year)	Sex	Symptom	Tumour location	Tumour site	Preoperative diagnosis
1	22	M	Cough, sputum	Central	Lt. LLB (B6)	Mucoepidermoid Ca.
2	40	W	Fever, chest pain	Central	Rt. MLB	Mucoepidermoid Ca.
3	58	W	Cough, sputum, fever	Central	Rt. BB (B9)	Non-typed malignant tumour
4	51	M	None	Peripheral	Rt. MLB (B4a)	No malignancy
5	37	W	Cough, sputum, fever	Central	Lt. UDB	No biopsy

Lt. LLB, Left lower lobe bronchus; Rt. BB, right basal bronchus; Rt. MLB, right middle lobe bronchus; Lt. UDB, left upper division bronchus.

ing patient was asymptomatic, and the lesion was detected during routine health examination.

The serum sialyl Lewis X-I antigen (SLX) values were high in all five cases. The serum carcinoembryonic antigen (CEA) and carbohydrate antigen 19-9 (CA19-9) values were high in three cases. The serum cytokeratin fragment 19 (CYFRA 21-1), squamous cell carcinoma antigen (SCC), neuron specific enolase (NSE), progastrin-releasing peptide (pro-GRP) values were all within the normal range.

3.2. HRCT findings

On the CT images, the tumours ranged in diameter from 18 to 38 mm (mean, 28.4 mm) (Table 2). The lesions were located in the central lung in four cases and in the peripheral lung in one. All the lesions were well defined nodules or masses with a smooth margin (Fig. 1). The contour of the tumours was round ($n = 1$), oval ($n = 3$) or lobulated ($n = 1$). Non-enhanced CT scans revealed intratumoral punctate calcification in one of the five lesions (Case 1). CT findings suggestive of bronchial stenosis or obstruction were seen in all cases (distal obstructive pneumonia in four cases, distal bronchial dilation in four and atelectasis in three). Atelectasis with recurrent or non-resolving pneumonia was observed distal to the site of obstruction.

CT attenuation coefficients were evaluated before and after administration of contrast medium. Thus, the change of CT attenuation or the degree of contrast enhancement was described. CT images enhanced by intravenous contrast medium showed marked heterogeneous enhancement with foci of relatively low attenuation in four of the five lesions and mild heterogeneous enhancement in the other lesion. Measurement of Hounsfield unit (HU) data was possible in every patient. The attenuation coefficients of the four markedly enhanced tumours (range, 95–139 HU; mean, 118.5 HU) were much higher than those of the chest wall musculature (range, 48–68; mean, 61.3 HU), whereas that of the one mildly enhanced tumour was slightly higher than that of the chest wall musculature. The ratio of the attenuation coefficient of the tumour to that of the musculature in the mildly enhanced case was 1.5, whereas those of the markedly enhanced cases were much higher (range, 2.0–2.2) (Table 2). None of the patients had lymphadenopathy in the mediastinum, pulmonary hilum or around the bronchi, on the basis of the CT findings.

3.3. Bronchoscopic findings

Bronchoscopy was performed in all five cases and the tumours were easily visualized except the peripheral lesion. The tumours were located in the lobar or segmental bronchi and had filled the bronchial lumen. They were soft, polypoid with a sessile base and pink like the bronchial mucosa. Three of the tumours were covered by a highly vascular mucosa. Although bronchoscopic brushing or biopsy was performed in four cases, a preoperative diagnosis of mucoepidermoid carcinoma was made in only two of them. Bronchoscopy in the other two cases revealed a non-typed malignant tumour or non-diagnostic inflammatory cells.

3.4. Treatment

The treatment chosen for all patients was surgical resection, and the procedure consisted of routine lobectomy including right middle and lower lobectomy (Table 2). The surgical procedures resulted in tumour-free margins. Lymph node dissection or sampling of pulmonary hilar and mediastinal lymph nodes was performed in all cases.

3.5. Histopathologic findings

The histologic diagnosis was low-grade mucoepidermoid carcinoma in all five cases (Table 3). The central tumours

Table 2 HRCT findings of mucoepidermoid carcinoma of the bronchus in four patients

Case	Tumour size (mm)	Tumour margin	Tumour contour	Pattern of enhancement	Ratio of attenuation coefficient
1	38 × 35	Well defined (smooth)	Oval	Heterogeneous	2.1
2	26 × 18	Well defined (smooth)	Lobulated	Heterogeneous	1.5
3	34 × 22	Well defined (smooth)	Oval	Heterogeneous	2.1
4	24 × 24	Well defined (smooth)	Round	Heterogeneous	2
5	33 × 29	Well defined (smooth)	Oval	Heterogeneous	2.2

Ratio of attenuation coefficient: Ratio of the attenuation coefficient of the tumour to attenuation coefficient of the musculature

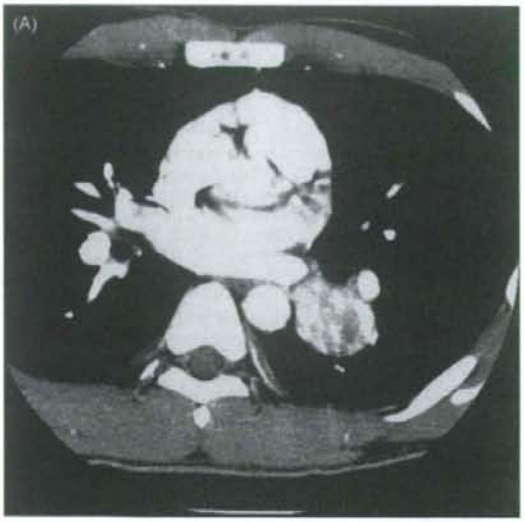

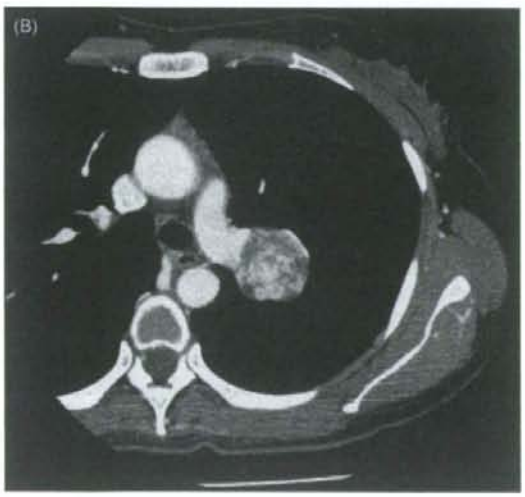

Fig. 1 Mucoepidermoid carcinomas of the bronchus were well defined mass and had a smooth margin. Enhanced CT images shows marked heterogeneous enhancement with foci of relatively low attenuation (A, Case 1; B, Case 5).

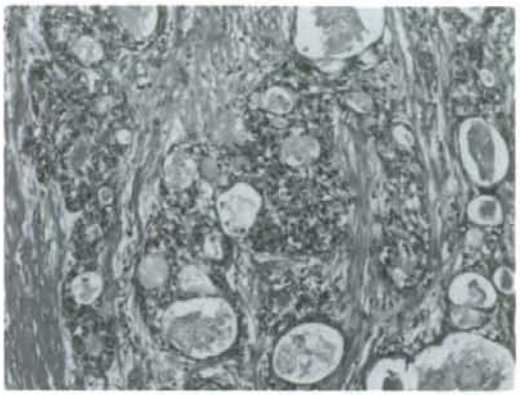

Fig. 2 High-magnification photomicrograph showed the epithelial component of the tumours consisted of mucin-secreting cells, squamoid cells and intermediate-type cells that displayed no specific differentiation.

protruded into the lumen of the bronchus and almost totally occluded it. On cut sections, the tumours were light yellow or tan polypoid masses. The margins and contours of the tumours were smooth, and they were well circumscribed and oval or round, consistent with their CT appearance.

Microscopically, the tumours were seen to arise from bronchial glands and to have infiltrated the bronchial wall. The epithelial component of the tumours consisted of mucin-secreting cells, squamoid cells and intermediate-type cells that displayed no specific differentiation (Fig. 2). Cystic change predominated in some areas, and the solid areas comprised mucin-secreting columnar epithelium that had formed small glands, tubules and cysts. There were no prominent nucleoli, and mitotic figures and necrosis were absent or minimal (less than five mitoses per 50 high-power fields). Keratinization was rare or absent in the epidermoid areas. These pathologic findings are characteristic of low-grade mucoepidermoid carcinoma. There was an admixed distribution of areas that are heterogeneous in the densities of blood vessels, as highlighted by immunohistochemical staining of CD31. Most mucin-secreting areas of the tumours showed more densely distributed blood vessels, mostly capillaries, in between tumour cell nests, whereas other areas did less (Fig. 3). Stromal calcification and ossification with a granulomatous reaction was observed in Case 1. The histologic specimens in Case 1, in which intratumoral punctate calcifications were observed on non-enhanced HRCT scans, showed microscopic calcification. Distal obstructive pneu-

Table 3 Histopathologic findings and outcome

Case	Treatment	p-Stage (TNM)	Grade	CD31	Outcome
1	Left lower lobectomy	T2N0M0 IB	Low-grade	(++)	NED
2	Right middle and lower lobectomy	T1N0M0 IA	Low-grade	(++)	NED
3	Right lower lobectomy	T2N0M0 IB	Low-grade	(+)	NED
4	Right middle lobectomy	T1N0M0 IA	Low-grade	(++)	NED
5	Light upper lobectomy	T2N0M0 IB	Low-grade	(++)	NED

NED: No evidence of disease.

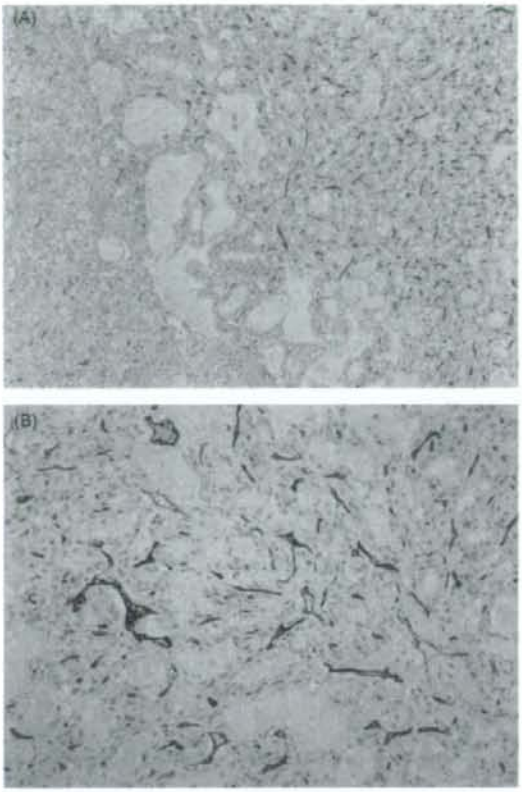

Fig. 3 (A) Immunohistochemical findings showing a border of areas with and without dense blood vessels as highlighted by anti-CD31 antibody. Note the abundant glands with mucus production in the right half, where there are more vessels labeled by anti-CD31 antibody. (B) Higher magnification of the area with plenty of mucin-secreting glands. Immunoreactive CD31 label the surface of endothelial cells, but not mucin of the tumour.

monia was observed in four patients with lesions of the central type, and distal bronchial dilation and mucoid impaction was seen in all five cases. The secondary findings associated with bronchial stenosis or obstruction on the HRCT scans largely reflected these pathologic findings. No lymph node metastasis was found in any of the surgical specimens.

4. Discussion

Mucoepidermoid carcinoma of the lung was first reported by Smetana et al. [11], and accounts for only a very small proportion of primary lung cancers. The tumours are classified as low grade or high grade based on their histologic appearance, and grading is based on cellular atypia, mitotic activity, local extension and tumour necrosis. Low-grade mucoepidermoid carcinoma is the most common type, and all five of the tumours in our series were low-grade. Although there is good clinicopathological evidence for the existence of the low-grade type, it has been questioned whether the high-grade type is a separate entity, mainly because of its histological similarity to mixed pulmonary carcinomas [5]. The high-grade variant is occasionally difficult to differentiate from adenosquamous carcinoma [12–14].

The most common symptoms are related to intraluminal growth, and these include persistent cough and sputum, wheezing, dyspnea, recurrent pneumonia, and, less frequently, hemoptysis [15]. Since the symptoms do not differ from those of other forms of lung tumour, they do not contribute to the differential diagnosis. Most patients with mucoepidermoid carcinoma are misdiagnosed as having bronchitis or lung carcinomas of other types. In our series, one patient was asymptomatic and the others had such similar symptoms that they were initially misdiagnosed as having chronic obstructive airway disease or other airway tumours.

Although the central-type tumours in our series were readily visible, only two of them were diagnosed preoperatively as mucoepidermoid carcinoma. Since mucoepidermoid carcinomas of the bronchi are usually covered by normal respiratory mucosa, bronchial brushing and lavage are seldom diagnostic, and it is better to perform a biopsy with forceps. Despite the theoretical risk of severe hemorrhage by performing a biopsy on a vascular mass, hemorrhage has never been reported as a complication of biopsy for mucoepidermoid carcinoma of the bronchus. Nevertheless, care is required because of the highly vascular nature of many of the tumours.

CT scan is non-invasive and useful for evaluating suspected endobronchial lesions, and fine morphological features have been revealed since the introduction of HRCT. In this series, HRCT images were essential for identifying the more detailed characteristics of the tumours, such as the margin, shape, density and pattern of enhancement. For the most part, the HRCT images reflected the pathologic features of the tumours well. There have been a few case reports of the HRCT appearance of mucoepidermoid carcinoma of the lung [7,10]. The HRCT features of the tumours in our series, such as a smooth margin and a well defined oval or round shape, were similar to those reported by Kim et al., who also found intratumoral punctate calcification on non-enhanced CT scans. Secondary findings associated with bronchial stenosis or obstruction, such as distal obstructive pneumonia, bronchial dilatation and atelectasis, were also seen. Although in their series Kim et al. reported mucoepidermoid carcinoma of the bronchus as showing mild contrast enhancement on CT scans, the three lesions of the central type and one lesion of the peripheral type in our series demonstrated marked contrast enhancement on HRCT images. The attenuation coefficients of the markedly enhanced tumours were much higher than those of the chest wall musculature.

Immunohistochemical staining for CD31 highlighted the heterogeneous distribution of blood vessels from mucin-secreting areas to non-secreting areas in a single tumour. In other words, these lesions may have characteristics of both hypervascular and hypovascular components, and the presence of both was probably the explanation for the features we observed on HRCT. The results of this study suggested that the presence of abundant microvessels, detected immunohistochemically by microscopic examination, affected the enhancement pattern on HRCT. These histopathologic findings correlated with the HRCT findings in all patients.

Bronchogenic carcinomas with more common histologic features, including adenocarcinoma, squamous cell carcinoma and small cell carcinoma have a variety of radiologic manifestations. Adenocarcinoma is often distinct from the other histologic subtypes of lung cancer. Non-solid nodules (ground glass opacities) and partly solid nodules (mixed solid/ground glass opacities) are recognized patterns of adenocarcinoma. Henschke et al. reported that the malignancies in subsolid nodules were typically bronchioloalveolar carcinomas or adenocarcinomas with bronchioloalveolar features, whereas in solid ones the malignancies were typically other subtypes of adenocarcinoma [16]. The proportion occupied by the non-solid component based on volumetric analysis by CT scan is a reliable predictor of tumours without vessel invasion in patients with adenocarcinoma of the lung [17]. Central squamous cell carcinoma is characterized by two major patterns of spread: intraepithelial spread with or without subepithelial invasion, and endobronchial polypoid growth. Polypoid tumours often occlude the bronchial lumen, resulting in atelectasis and obstructive pneumonia. Peripheral squamous cell carcinomas are seen as solid nodules, occasionally with cavitation and irregular margins. Approximately 90–95% of all small cell lung cancers are located centrally and show mediastinal or hilar lymphadenopathy with displacement or narrowing of the tracheobronchial tree or major vessels [18]. These common histologic types of lung cancer usually show mild or less contrast enhancement on CT images. Since these CT findings in common forms of lung carcinoma differ from those of mucoepidermoid carcinoma, which are relatively characteristic, contrast-enhanced CT may be helpful for lesion characterization and tumour classification in affected patients. If a marked heterogeneous contrast enhancement pattern is observed in well circumscribed oval or round masses of the bronchus, mucoepidermoid carcinoma can be considered in the differential diagnosis.

Large cell neuroendocrine carcinoma shows non-specific CT findings similar to those of other non-small cell lung cancer. On contrast-enhanced CT scans, tumour attenuation varies from slightly less to more than that of the chest wall muscle, with a homogeneous or heterogeneous pattern [18,19]. However, large cell neuroendocrine carcinoma is more likely to appear in the peripheral lung. Adenosquamous carcinoma of the peripheral type also usually shows heterogeneous soft-tissue attenuation [20]. Histopathologically, adenosquamous carcinoma is occasionally difficult to differentiate from high-grade mucoepidermoid carcinoma, which invades the pulmonary parenchyma in nearly 46% of the cases [3,12–14].

Pulmonary carcinoid tumours, which are low-grade malignancies accounting for 2–3% of all lung neoplasms [21], show CT findings similar to those of mucoepidermoid carcinoma. Pulmonary carcinoid tumours are also known to be vascular, and often show marked contrast enhancement on CT images [18,22]. Therefore, it is difficult to differentiate pulmonary carcinoid tumour from mucoepidermoid carcinoma on the basis of the CT contrast enhancement pattern alone.

Follow-up information was available for all five of the present cases. The clinical course of the patients was correlated with the histologic grade of their tumours. Low-grade mucoepidermoid carcinoma generally grows locally and is amenable to complete surgical resection. Low-grade tumours spread to regional lymph nodes by local growth in less than 5% of cases, and distant spread is rare [3,15]. The prognosis of low-grade tumours is usually excellent, with no evidence of local recurrence or metastasis. However, Barsky et al. [23] reported cases that were diagnosed as well differentiated and low-grade malignancy histologically but were rated as high-grade malignancy clinically. It can therefore be concluded that the histologic malignancy level of the tumour is not always the same as its clinical malignancy level. This suggests that complete surgical resection plus lymph node dissection should be performed for low-grade mucoepidermoid carcinoma of the bronchus as well as high-grade mucoepidermoid carcinoma. All five patients in our series underwent lobectomy plus lymph node dissection or sampling, and all are currently alive without evidence of disease at an average of 50.4 months after surgery (range, 15–82 months; median, 57 months).

5. Conclusions

We reviewed the HRCT and pathologic findings in five cases of mucoepidermoid carcinoma of the lung. Mucoepidermoid carcinoma is often visualized as marked heterogeneous contrast enhancement on HRCT images. The presence of abundant microvessels, detected immunohistochemically by microscopic examination, may affect the enhancement pattern on HRCT. However, examinations of HRCT images of mucoepidermoid carcinoma of the lung are insufficient because of the rarity of the tumour. The HRCT characteristics of the tumour must therefore be evaluated in more cases.

Conflict of interest

None declared.

References

[1] Colby TV, Koss MN, Travis WD. Tumors of salivary gland type. Tumors of the lower respiratory tract: AFIP atlas of tumor pathology 3rd series, vol. 13. Washington, DC: American Registry of Pathology; 1995. p. 65–89.
[2] Spencer H. Bronchial mucous gland tumours. Virchows Arch A Pathol Pathol Anat 1979;383:101–15.
[3] Yousem SA, Hochholzer L. Mucoepidermoid tumors of the lung. Cancer 1987;60:1346–52.
[4] Miller DL, Allen MS. Rare pulmonary neoplasms. Mayo Clin Proc 1993;68:492–8.
[5] Klacsmann PG, Olson JL, Eggleston JC. Mucoepidermoid carcinoma of the bronchus: an electron microscopic study of the low grade and the high grade variants. Cancer 1979;43:1720–33.
[6] Heitmiller RF, Mathisen DJ, Ferry JA, Mark EJ, Grillo HC. Mucoepidermoid lung tumors. Ann Thorac Surg 1989;47:394–9.
[7] Kim TS, Lee KS, Han J, Im JG, Seo JB, Kim JS, et al. Mucoepidermoid carcinoma of the tracheo-bronchial tree: radiographic and CT findings in 12 patients. Radiology 1999;212:643–8.
[8] Fisher DA, Mond DJ, Fuchs A, Khan A. Mucoepidermoid tumor of the lung: CT appearance. Comput Med Imaging Graph 1995;19:339–42.

[9] Tsuchiya H, Nagashima K, Ohashi S, Takase Y. Childhood bronchial mucoepidermoid tumors. J Pediatr Surg 1997;32:106–9.
[10] Kinoshita H, Shimotake T, Furukawa T, Deguchi E, Iwai N. Mucoepidermal carcinoma of the lung detected by positron emission tomography in a 5-year-old girl. J Pediatr Surg 2005;40:E1–3.
[11] Smetana HF, Iverson L, Swan LL. Bronchogenic carcinoma. Analysis of 100 autopsy cases. Milit Surg 1952;3:335–51.
[12] Leonardi HK, Jung-Legg Y, Legg MA, Neptune WB. Tracheobronchial mucoepidermoid carcinoma: clinicopathological features and results of treatment. J Thorac Cardiovasc Surg 1978;76:431–8.
[13] Stafford JR, Pollock J, Wenzel BC. Oncocytic mucoepidermoid tumor of the bronchus. Cancer 1984;54:94–9.
[14] Stafford JR, Pollock J, Wenzel BC. Bronchial mucoepidermoid carcinoma metastatic to skin. Report of a case and review of the literature. Cancer 1986;58:2556–9.
[15] Granata C, Battistini E, Toma P, Balducci T, Mattioli G, Fregonese B, et al. Mucoepidermoid carcinoma of the bronchus. Paediatr Pulmonol 1997;23:226–32.
[16] Henschke CI, Yankelevitz DF, Mirtcheva R, McGuinness G, McCauley D, Miettinen OS, et al. CT screening for lung cancer: frequency and significance of part-solid and nonsolid nodules. AJR Am J Roentgenol 2002;178:1053–7.
[17] Tateishi U, Uno H, Yonemori K, Satake M, Takeuchi M, Arai Y. Prediction of lung adenocarcinoma without vessel invasion: a CT scan volumetric analysis. Chest 2005;128:3276–83.
[18] Chong S, Lee KS, Chung MJ, Han J, Kwon OJ, Kim TS. Neuroendocrine tumors of the lung: clinical, pathologic, and imaging findings. Radiographics 2006;26:41–57.
[19] Oshiro Y, Kusumoto M, Matsuno Y, Asamura H, Tsuchiya R, Terasaki H, et al. CT findings of surgically resected large cell neuroendocrine carcinoma of the lung in 38 patients. AJR Am J Roentgenol 2004;182:87–91.
[20] Yu JQ, Yang ZG, Austin JH, Guo YK, Zhang SF. Adenosquamous carcinoma of the lung: CT-pathological correlation. Clin Radiol 2005;60:364–9.
[21] Davila DG, Dunn WF, Tazelaar HD, Pairolero PC. Bronchial carcinoid tumors. Mayo Clin Proc 1993;68:795–803.
[22] Fauroux B, Aynie V, Larroquet M, Boccon-Gibod L, Ducou le Pointe H, Tamalet A, et al. Carcinoid and mucoepidermoid bronchial tumours in children. Eur J Pediatr 2005;164:748–52.
[23] Barsky SH, Martin SE, Matthews M, Gazdar A, Costa JC. "Low grade" mucoepidermoid carcinoma of the bronchus with "high grade" biological behavior. Cancer 1983;51:1505–9.

Carcinogenesis vol.29 no.5 pp.957–963, 2008
doi:10.1093/carcin/bgn048
Advance Access publication February 24, 2008

Association of KRAS polymorphisms with risk for lung adenocarcinoma accompanied by atypical adenomatous hyperplasias

Takashi Kohno[1], Hideo Kunitoh[2], Kenji Suzuki[3], Seiichiro Yamamoto[4], Aya Kuchiba[4,5], Yoshihiro Matsuno[6,8], Noriko Yanagitani[1,7] and Jun Yokota[1,*]

[1]Biology Division, National Cancer Center Research Institute, Tokyo 1040045, Japan, [2]Thoracic Oncology Division, [3]Thoracic Surgery Division, National Cancer Center Hospital, Tokyo 1040045, Japan, [4]Cancer Information Services and Surveillance Division, Center for Cancer Control and Information Services, National Cancer Center, Tokyo 1040045, Japan, [5]Department of Biostatistics/Epidemiology and Preventive Health Sciences, Graduate School of Medicine, The University of Tokyo, Bunkyo-ku, Tokyo 1130033, Japan, [6]Diagnostic Pathology Division, National Cancer Center Hospital, Tokyo 1040045, Japan and [7]First Department of Internal Medicine, Gunma University School of Medicine, Showa-machi, Gunma 3718511, Japan

[8]Present address: Department of Surgical Pathology, Hokkaido University Hospital, Sapporo 0608648, Japan

*To whom correspondence should be addressed. Tel: +81 3 3542 2511; Fax: +81 3 3542 0807;
Email: jyokota@gan2.ncc.go.jp.

The *pulmonary adenoma susceptibility 1* (*Pas1*) gene affects susceptibility to the development of lung adenomas in mice with a subset of the adenomas progressing to adenocarcinoma (ADC). In this study, genotype distributions for 10 polymorphisms in the human counterparts for three mouse candidate *Pas1* genes, *KRAS*, *CASC1*/*LAS1* and *LRMP*, were examined in a hospital-based case–control study consisting of 364 lung ADC cases and 253 controls. All the ADC cases were subjected to lobectomy and subsequent pathological investigation of atypical adenomatous hyperplasia (AAH), a putative precursor for peripheral lung ADC, including bronchioloalveolar carcinoma, in the resected lobes. Eighty-one (22%) of the ADC cases carried at least one AAH lesion in addition to the primary ADC and 34 (9%) of them carried multiple AAH lesions. None of the 10 polymorphisms examined showed significant associations with overall lung ADC risk ($P > 0.05$). However, minor allele carriers for two polymorphisms in the *KRAS* gene, KRAS-1 and -6, showed significantly increased odds ratios (ORs) for ADC accompanied by multiple AAHs [OR = 3.0; 95% confidence interval (CI) = 1.4–6.2, $P = 0.004$ and OR = 2.4; 95% CI = 1.1–4.7, $P = 0.02$, respectively]. Minor haplotypes including the minor allele for the KRAS-6 polymorphism showed increased ORs for ADC accompanied by multiple AAHs, and *KRAS* transcripts from the minor allele for this polymorphism were more abundantly detected in lung tissues than those from the major allele. Thus, *KRAS* polymorphisms were indicated to be involved in risk for the development of AAHs that progress to ADC by causing differential *KRAS* oncogene expression in the lungs.

Introduction

Adenocarcinoma (ADC) is now the most common type of non-small cell lung carcinoma, followed by squamous cell carcinoma and small cell carcinoma (1,2). Development of lung ADC is less associated with smoking compared with squamous cell carcinoma and small cell carcinoma. Thus, effective ways of preventing ADC are being searched for (1,2). Identification of genes responsible for susceptibilit to lung ADC is considered to be indispensable to establish novel an efficient ways of preventing the disease. However, only a few meta bolic and DNA repair genes, such as *CYP1A1* and *OGG1*, have bee shown to be associated with risk for lung ADC (1,3–6), and therefor genes responsible for lung ADC susceptibility are largely unknown

Inbred strains of mice exhibit a difference in their susceptibilitie to both spontaneous and carcinogen-induced lung adenoma devel opment (7). To date, dozens of genetic loci have been shown to b linked to mouse lung adenoma susceptibility (*Las*) through linkag analyses, including pulmonary adenoma susceptibility (*Pas*), pulmo nary adenoma resistance and susceptibility to lung cancer (8–12 Recently, we reported that a non-synonymous (associated wit amino acid change) single-nucleotide polymorphism (SNP) in *PO LI*, the human counterpart for a candidate pulmonary adenoma re sistance 2 gene, was associated with lung ADC risk (13). Thus, i was suggested that human counterparts for mouse *Las* genes als play a role in human lung ADC risk. *Pas1* is a major locus account ing for ~50% of variances in *Las* in mice, and three genes of Kirste rat sarcoma oncogene (*Kras*) 2, cancer susceptibility candidat (*Casc*) 1/*Las1* and lymphoid-restricted membrane protein (*Lrmp* have been identified from this locus as strong candidates determin ing the susceptibility (11,14–18). A case–control study of lung AD in an Italian population showed that a SNP in the *KRAS* gen (KRAS-1 in Table I) was associated with lung ADC risk (19); how ever, the association was not reproduced in the following studie (20,21). SNPs in the *LRMP* and *CASC1* genes did not show associ ations with lung ADC risk in a recent study (22). Instead, the abov SNP in *KRAS* and a SNP in *LRMP* (LRMP-6 in Table I) showe associations with prognosis of lung ADC patients (19,20,22). Thus it is still controversial how the human counterparts for the mous *Pas1* genes are involved in the development and progression of lun ADC in humans.

The mouse *Pas1* gene affects susceptibility to lung adenoma de velopments in mice, and a subset of the adenomas progress to AD that is analogous to bronchioloalveolar carcinoma (BAC) in human (7). Thus, it is possible that variations in human counterparts fo *Pas1* are also involved in susceptibility to the development of lun adenoma and/or BAC (18). Atypical adenomatous hyperplasi (AAH) is a lesion with a monoclonal nature (23) and has bee considered as a precursor for peripheral lung ADC, includin BAC, the adenoma in an adenoma–carcinoma sequence in the pe ripheral lung (24). AAH is a frequent incidental histologic finding i lungs bearing primary lung ADC (24,25). Such an accompanimer of AAH was detected in 16–35% of ADC cases. AAH was als detected in the lungs of autopsy cases without cancer by histologic examination. In two studies, AAH was examined in hospital autops cases and was detected in 2.0 and 3.4% of the cases without cance respectively (26,27). In another study, administration autopsy case were examined to estimate the prevalence of AAH in the gener population, and AAH was detected in 2.8% of the cases (28). There fore, AAH is indicated to be present in the lungs of individual without cancer; however, the frequency of having AAH in thos individuals is considerably lower than that in ADC patients (24 The results indicate that the susceptibility to the development c AAH is also associated with that of lung ADC in humans, an therefore, the lungs of humans with primary ADCs accompanie by AAH, particularly those accompanied by multiple AAHs, ar analogous to those of mice with the susceptible *Pas1* allele. Thus in the present study, polymorphisms of the *KRAS*, *CASC1* and *LRM* genes were examined for association with risk for the developmer of lung ADC after subclassification of the subjects according t AAH accompaniment and BAC component involvement.

Abbreviations: AAH, atypical adenomatous hyperplasia; ADC, adenocarcinoma; BAC, bronchioloalveolar carcinoma; Casc, cancer susceptibility candidate; cDNA, complementary DNA; CI, confidence interval; *Kras*, Kirsten rat sarcoma oncogene; *Las*, lung adenoma susceptibility; LD, linkage disequilibrium; LRMP, lymphoid-restricted membrane protein; OR, odds ratio; *Pas1*, pulmonary adenoma susceptibility 1; PCR, polymerase chain reaction; SNP, single-nucleotide polymorphism.

Table I. Ten polymorphisms in the KRAS, CASC1 and LRMP genes, and primers and conditions for pyrosequencing

Polymorphism	Accession no. in dbSNP	Nucleotide substitution[a]	Location	Amino acid change	PCR			Sequencing
					Forward primer (5′ → 3′)	Reverse primer (5′ → 3′)	Annealing temperature (°C)	Primer
KRAS								
12	rs2955407	A/G	Gene upstream		AACATGGGGAATTTGGCTTT	TTCACAGGCACTTCATTCTCA	63	TTGGACAGGCATTTG
1[b]	rs11836509	A/C	Intron 3		GAGTCTTTGCTAATGCCATGC	CACTGCTCTAATCCCCCAAG	61	TGCCATGCATATAATATTT
6	-/T		Exon 4b (3′-UTR)		GGCCATACTTCAGGAACTGC	TTTGTTAAACCATTCAAAGTTCACA	63	GGGCATTTTTTTAAGGTAG
CASC1								
1[b]	rs10842501	A/G	Intron 1		AACTTTTAGGGTCCCAAAGC	CTGTTCATACACTGTAAGTG	55	GTTCATACACTGTAAGTGAT
4[b]	rs10842496	C/A	Exon 3	Arg33Ser	AAATTATTTTTGGTTCTTTAGAGGAAG	GCTTCAAGTCGATGCCATTT	55	GGTTCTTTAGAGGAAGCC
5	rs2352782	T/C	Intron 8		AAGAAGACCTTTCGTACTTACCAG	TGGGGTATAACCCCTTGTCA	61	TCGTACTTACCAGTGCAT
LRMP								
7[b]	rs1908946	C/G	Exon 13	Ser197Cys	AGAGAGGTCCCGTGACTTGG	CCCAAATGTTCTGATTCTCACC	61	ATTTGAAGAAAGAAATCACT
6[b]	rs7969931	G/C	Exon 11	Val141Leu	GTGGTTTCCCCTCTTCCTGT	CATGCTACATGAAGAAGCACTTA	61	TTACTTCTCACTTTGTCTAA
4	rs2291801	C/T	Intron 5		AGTTGGTGCGTGCTGGTTAT	TCCACATTTGGGCTCTTTTC	61	TGCTGGTTTAAATAGAGG
1	rs1497259	G/A	Intron 1		CTTCACGGCCCAATAGATTC	TTTGGGCAGCAAAAGATACA	61	GGCAGCAAAAGATACAA

[a]Shown in the direction of genes.
[b]Association with lung ADC risk was examined in previous studies.

Materials and methods

Case and control subjects

All cases and controls were Japanese. The cases consisted of 364 ADC patients treated at the National Cancer Center Hospital, Tokyo. All ADC cases, who received lobectomies from 1999 to 2004 and from whom informed consents as well as blood samples were obtained, were consecutively included in this study without any particular exclusion criteria. All the cases were diagnosed as ADC by histological examinations according to the World Health Organization classification (24,29). Information on the AAH in the ADC patients was obtained by routine surgical pathology examination as follows. Resected lungs were inflated with 10% formalin through bronchial cut ends and after fixation for a few days were serially sliced at intervals of 5 mm, and each cut surface was macroscopically examined. Sliced lungs containing a lesions suspected for AAH were further examined microscopically. Even in cases without macroscopic lesions, at least one tissue block was prepared from all sliced lungs and subjected to microscopic examination. The criteria for AAH were as follows as described previously (27,28): (i) a localized lesion with well-defined boundaries; (ii) an alveolar wall slightly thickened with mild infiltration of inflammatory cells but without scar formation; (iii) proliferating atypical epithelial cells abutting each other but not as compact as in ADC; (iv) atypical epithelial cells that were cuboidal to low columnar or peg shaped in appearance, resembling either type II pneumocytes or non-ciliated bronchiolar epithelial cells (Clara cells) and (v) the presence of some atypical cells with two or more nuclei, most of which had relatively smaller and smoother contours than those of ADC. These criteria are compatible with those described in the reference of World Health Organization classification of lung tumors as a proposal (24,30). The controls consisted of cancer-free patients of National Cancer Center Hospital. All the control subjects were selected with a criterion of no history of cancer. Smoking history of cases and controls was obtained via interview using a questionnaire. Smoking habit was expressed by pack-years, which was defined as the number of cigarette packs smoked daily multiplied by years of smoking, both in current smokers and former smokers. Smokers were defined as those who had smoked regularly for 12 months or longer at any time in their life, whereas non-smokers were defined as those who had not. From each individual, a 20 ml whole-blood sample was obtained. The study was approved by the Institutional Review Boards of the National Cancer Center.

DNA extraction, polymorphism search and genotyping

Genomic DNAs were isolated from whole-blood samples using a QIAamp DNA Blood Maxi kit (Qiagen, Tokyo, Japan). DNAs from 24 lung ADC cases and 24 controls, respectively, were subjected to a search for polymorphisms in exons of the *KRAS*, *CASC1* and *LRMP* genes by resequencing according to the procedure described previously (13). SNPs in introns of these three genes with minor allele frequencies >0.1 in the Japanese population were selected from SNPs deposited in the dbSNP database (http://www.ncbi.nlm.nih.gov/projects/SNP/). Genotyping was performed with 10 ng of genomic DNA by the pyrosequencing method according to the procedure described previously (13).

Statistical analysis

Hardy–Weinberg equilibrium tests were performed using the SNPAlyze version 3 software (DYNACOM Co., Ltd, Chiba, Japna). SNPs with a P value for deviation >0.01 were considered to be in Hardy–Weinberg equilibrium. Calculation of the D' values and haplotype estimation were undertaken using the expectation-maximization (EM) algorithm using the same software. The strength of association of genotypes with ADC risks was measured as crude odds ratios (ORs) and ORs adjusted for gender, age (<49, 50–59, 60–69 and >70) and smoking dosage (pack-years: 0, 1–49 and >50) with 95% confidence intervals (CIs) by unconditional logistic regression analysis (31). Statistical analyses were performed using the JMP version 6.0 software (SAS Institute, Cary, NC). ORs for carrying a copy of a haplotype were also calculated by the bootstrap method with 5000 resampling. The statistical analyses were performed using the SAS version 9 software (SAS Institute). Statistically, a level of $P < 0.05$ for an OR was considered significant, whereas a level of $0.05 \leq P < 0.10$ for an OR was considered marginally significant.

Analysis of KRAS transcripts

Genomic DNA and total RNA were extracted from eight non-cancerous lung tissues of eight lung ADC patients heterozygous for an insertion–deletion polymorphism, KRAS-6 (see Table I). Complementary DNA (cDNA) was synthesized by reverse transcription of 1 mg of total RNA using the Superscript First-Strand Synthesis System. Ten nanograms of genomic DNA and cDNA corresponding to 50 ng of total RNA were subjected to polymerase chain reaction (PCR) in duplicate. The PCR was performed using a set of primers, 5′-CAGGAACTGCAGTGCTTATG-3′ and 5′-TTAAGGCTGTAATAATTAGGTAAC-3′ (fluorescein isothiocyanate labeled), for 30 cycles consisting of

denaturation at 95°C for 1 min, annealing at 60°C for 1 min and extension at 72°C for 1 min. PCR products were electrophoresed using an ABI PRISM 3700 Genetic Analyzer and analyzed by Gene Scan software (Applied Biosystems, Foster City, CA). Ratios of the minor allele (i.e. T allele) to the major allele (i.e. – allele) products in each sample were calculated from the height of peaks corresponding to the minor and major alleles, respectively. The ratio for each sample was expressed by the mean ratios of the two independent PCRs. The difference in the mean ratios between genomic DNA and cDNA in eight cases was tested by the paired *t*-test.

Results

We searched for polymorphisms located in exons of the *KRAS*, *CASC1* and *LRMP* genes by the resequencing of their exons in 48 Japanese individuals, and identified a 1 bp insertion–deletion polymorphism in the *KRAS* gene and three non-synonymous SNPs in the *CASC1* and *LRMP* genes (Table I). The insertion–deletion polymorphism was novel, while the three SNPs had been deposited in the dbSNP database. Six other SNPs in introns of these three genes whose minor allele frequencies were >0.1 in the Japanese population were selected from SNPs deposited in the dbSNP database (Table I). In total, 10 polymorphisms dispersed in the *KRAS*, *CASC1* and *LRMP* genes were selected for the present study (Figure 1).

We prepared 364 ADC cases and 253 hospital-based controls (Table II). The ADC cases received lobectomies at National Cancer Center Hospital and were subjected to the pathological search for AAH in the resected lobes. In the lobes, one or more (i.e. multiple) AAH lesions were detected in 81 cases (22%), while no AAH lesion was detected in the remaining 283 cases (78%). The frequency of AAH accompaniment in these ADC cases was consistent with those in previous studies (24). Representative microphotographs of multiple AAH lesions detected in an ADC patient are shown in supplementary Figure 1 (available at *Carcinogenesis* Online). In 34 of the 81 cases (9%), 2 or more (i.e. multiple) AAH lesions were detected. The 364 ADC cases included 173 cases of small-sized ADC (i.e. <2 cm in maximum diameter), and the information on the presence of BAC components in the tumor was available (Table II). One hundred and fifty-two cases (88%) contained BAC components in the tumor, whereas the remaining 21 cases (12%) did not. It was difficult to histologically define AAHs in primary ADC lesions, even in ADCs with BAC components. Thus, it was not possible to pick up cases of ADCs in AAH lesions, so-called 'carcinoma in adenoma'. Accordingly, cases with AAHs were defined as having AAHs that existed independently from primary ADCs in the present study.

All the cases and controls were subjected to genotyping for the 10 polymorphisms, and all the polymorphisms were in Hardy–Weinberg equilibrium both in the cases and controls. Genotypic differentiation for the 10 polymorphisms was examined between cases and controls. The differentiation was examined for all ADC cases as a whole and cases categorized by AAH accompaniment. The differentiation wa also examined for small-sized ADC cases with BAC components. Th number of small-sized ADC cases without BAC components wa small; therefore, they were excluded from the analysis. The differen tiation was also examined after dividing ADC subjects into smoker and non-smokers. To increase statistical power, genotypic differenti ation was examined by assessing OR of minor allele carriers agains homozygotes for the major allele (i.e. non-carriers).

Minor allele carriers for a SNP, KRAS-12, showed a marginall significant increase in the OR for the risk for overall ADC ($P = 0.06$, while none of the other nine polymorphisms showed significant in creases or decreases in the OR (Table III). When the ADC cases wer categorized by AAH accompaniment, ORs of minor allele carriers fc six polymorphisms, KRAS-1, -6, CASC-1, -4, -5 and LRMP-7 against non-carriers were higher for ADC with AAH than for tha without. The ORs were even higher for ADC with ≥2 AAHs. In creases in adjusted ORs for two of the six polymorphisms, KRAS- and -6, were statistically significant (OR = 3.0; 95% CI = 1.4–6. and 2.4; 95% CI = 1.1–5.1, respectively), and those for three othe polymorphisms, CASC-1, -4 and LRMP-7, were marginal (Table III

We next calculated ORs for the risk for small-sized ADC with BA components. Minor allele carriers for the KRAS-1 SNP, whic showed the most significantly increased OR of 1.3 for ADC wit ≥2 AAHs, showed a slightly increased OR against non-carriers fc the risk for ADC with BAC components, but the increase was nc statistically significant ($P = 0.3$) (Table III). ORs for the other nin polymorphisms were not significant, either. When the ADC case were divided into smokers and non-smokers, ORs were not apparentl different between them. Increases or decreases in ORs were not sig nificant, either.

Linkage disequilibrium (LD) among the 10 polymorphisms wa then estimated. Five polymorphisms, KRAS-1, -6, CASC1-1, -4 an -5, were in LD with one another ($D' > 0.9$) (Figure 1), and the size c the region with LD was 94 kb. Thus, the distribution of haplotype consisting of these five polymorphisms was evaluated in cases an controls (Table IV). Three haplotypes were deduced to compris ~97% of chromosomes among controls and cases. The major haplc type consisting of major alleles for all the five polymorphisms (i.e haplotype 1 in Table IV) was less prevalent in ADC cases with ≥ AAHs than in controls, whereas a minor haplotype consisting c minor alleles for the five polymorphisms (i.e. haplotype 2) was mor prevalent. Haplotype 3 was almost evenly distributed in cases an controls. Adjusted ORs for the risk for ADC accompanied by ≥ AAHs by carrying one copy of haplotypes 2 and 3 was calculate based on the estimated copy number of haplotypes for each subject b the bootstrap method. The ORs for haplotypes 2 and 3 were 2.6 (95% CI = 1.1–5.9, $P = 0.02$) and 1.8 (95% CI = 0.6–5.6, $P = 0.3$), re spectively. Therefore, both haplotypes showed increased ORs, whil only increase in the OR for haplotype 2 was statistically significant

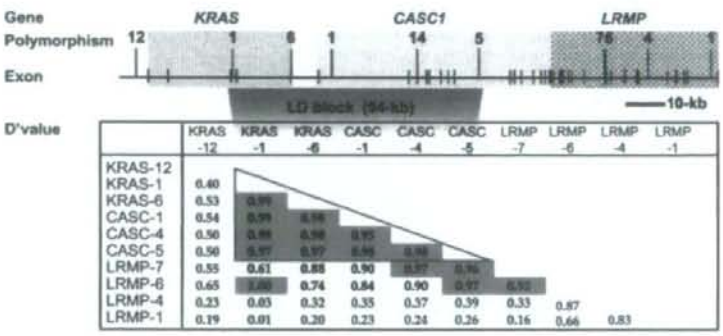

Fig. 1. Polymorphisms in the human *Pas1* locus and their LD. Ten polymorphisms are shown on top, and D' values between the SNPs are shown below. D' values >0.9 are marked in red.

Table II. Lung ADC cases and controls used in this study

Subject and category	All	Sex (%)		Age	Smoking habit (%)[a]	
		Male	Female	(Mean ± SD)	Smoker	Non-smoker
Case	364 (100)	196 (54)	168 (54)	61 ± 10	174 (48)	189 (52)
AAH accompaniment						
Absent	283 (77)	157 (55)	126 (45)	62 ± 11	135 (48)	147 (52)
Present	81 (23)	39 (48)	42 (52)	61 ± 8	36 (44)	45 (56)
1 AAH	47 (14)	20 (43)	27 (57)	61 ± 8	22 (47)	25 (53)
≥2 AAHs	34 (9)	19 (56)	15 (44)	62 ± 7	14 (41)	20 (59)
Tumor size						
≤2 cm	173 (47)	94 (54)	79 (46)	61 ± 10	93 (54)	79 (45)
BAC component (+)	152 (41)	83 (55)	69 (45)	61 ± 10	85 (56)	66 (43)
BAC component (−)	21 (6)	11 (52)	10 (48)	61 ± 11	8 (38)	13 (62)
>2 cm	191 (53)	114 (60)	77 (40)	62 ± 10	110 (58)	81 (42)
Control	253 (100)	144 (57)	109 (43)	64 ± 11	134 (53)	117 (46)

[a]Data were not available for one case and two control subjects.

In mice, it was shown that *KRAS* transcripts from the susceptible *Pas1* allele in lung tissue are more abundant than those from the resistant allele, and such a difference was proposed to underlie the difference in the susceptibility to adenoma development (18). As described above, hapolytypes 2 and 3, which showed significantly and insignificantly increased ORs for ADC accompanied by multiple AAHs, respectively, contained a minor allele for KRAS-6, a 1 bp insertion–deletion polymorphism in the 3′-untranslated region (3′-UTR) of the *KRAS* gene. This result prompted us to compare the amounts of *KRAS* transcripts between susceptible and resistant alleles by using the KRAS-6 polymorphism. Genomic DNA and cDNA prepared from non-cancerous lung tissues of eight heterozygotes for this polymorphism were subjected to PCR using a set of primers that amplifies the same DNA/cDNA fragments encompassing the KRAS-6 site. Relative amounts of the susceptible (i.e. T) allele products to the resistant (i.e. −) allele products were greater in cDNA than in genomic DNA in all the eight cases (Figure 2). The mean for the ratio of the minor allele products to the major allele products in genomic DNA and cDNA was 1.02 and 1.13, respectively, and the difference was statistically significant ($P = 0.005$ by the paired *t*-test). Thus, it was indicated that transcripts from the KRAS-6 minor allele were more abundant than those from the major allele in lung tissues.

Discussion

In the present study, we examined the association of polymorphisms in the human counterparts for three mouse candidate *Pas1* genes with risk for lung ADC. None of the 10 polymorphisms examined showed significant associations with risk for lung ADC as a whole. This result was consistent with recent case–control studies (20,22). However, when ADC subjects were categorized according to AAH accompaniment, two polymorphisms, KRAS-1 and -6, showed associations with risk for ADC accompanied by multiple AAHs. Haplotypes containing the minor allele for the KRAS-6 polymorphism also showed increased ORs for ADC accompanied by multiple AAHs. The results strongly suggested that *KRAS* is a determinant for susceptibility to ADC accompanied by multiple AAHs in humans. Namely, individuals with minor alleles for these two *KRAS* polymorphisms could have a higher risk than those without for the development of lung tumors analogous to the tumors in mice with a susceptible *Pas1* allele; i.e. multiple adenomatous lesions (multiple AAHs) with a subset of lesions that have progressed to primary ADC. *KRAS* transcripts from the risk haplotypes were more abundant than those from the resistant haplotype. This result was also analogous to the status of the mouse *Pas1* locus (18). *KRAS/Kras* is an oncogene that is activated by somatic mutations in lung ADC both of humans and mice (32–35). Thus, an abundant *KRAS/Kras* expression due to polymorphisms might make the lung epithelial cells more susceptible to the development of adenomas, a subset of which progress to ADC, both in humans and mice.

KRAS minor allele carriers showed only a slightly increased and insignificant OR for the risk for development of lung ADC as a whole and even of lung ADC with BAC components, which is considered to develop from AAH. This result is in contrast to the finding in mice that *Pas1* has a major role in predisposition to not only lung adenoma but also lung ADC (36). The result may imply that *KRAS* polymorphisms are responsible for the development of AAH; however, their effects on the development of lung ADC, including BAC, are limited. In this context, however, we should consider the difference in the process of ADC development between mice and humans. In the studies of experimental mouse models, lung ADCs in mice could be exclusively developed through adenomas; therefore, *Pas1* might have been judged as having a role in the predisposition to not only lung adenoma but also lung ADC. In humans, in contrast, a subset of ADC, including BAC, may not be developed through AAH. This could be a reason why the *KRAS* minor allele has not been defined as a risk allele for lung ADC development in several studies, including this one. In fact, fractions of minor allele carriers for KRAS-1 and -6 polymorphisms in ADC cases with multiple AAHs were significantly higher than those in ADC cases without AAH (OR = 3.0; 95% CI = 1.4–6.2, $P = 0.004$ and OR = 2.2; 95% CI = 1.1-4.7, $P = 0.03$, respectively). This result further supports that *KRAS* polymorphisms are responsible for the development of AAH but not of lung ADC. In addition, progression of AAH to ADC in mice can be influenced by several other genetic factors, as indicated by the pulmonary adenoma progression loci, which determine the susceptibility to the progression of adenoma to ADC in the lungs (21,36). Thus, association of polymorphisms in the *KRAS* gene with risk for lung AAH and ADC should be further examined in a larger number of samples in conjunction with polymorphisms of human counterparts for such modifier loci for *Pas1*.

Two SNPs in the *KRAS* gene were in LD with three other SNPs in a nearby gene, *CASC1*. A haplotype consisting of minor alleles of these five polymorphisms were significantly associated with risk for ADC with multiple AAHs. Genotypes with minor alleles for polymorphisms of the *CASC1* gene also showed increased ORs for ADC accompanied by multiple AAHs, although they were not statistically significant. Thus, it was also suggested that *CASC1* polymorphisms could also be involved in the susceptibility to ADC with multiple AAHs. Similar results were also shown in mice; *Casc1* polymorphisms are in LD with *KRAS* polymorphisms, and *Casc1* polymorphisms also showed associations with lung adenoma risk (14,15,37). The *Casc1* gene has a polymorphism associated with amino acid substitution. Casc1 protein has a growth-suppressive activity on lung cancer cells, and the activity was indicated to be different between the polymorphic proteins (15). However, differential expression of *Casc1* was not observed between polymorphic alleles (18). Thus, it is

Table III. KRAS, CASC1 and LRMP genotypes and risks for ADC

SNP	Genotype	Control	Case												
			All			AAH accompaniment									
						Absent			Present						
									All			1 AAH			≥2 AAHs		
		No. (%)	No. (%)	OR[a]	P	No. (%)	OR[a]	P	No. (%)	OR[a]	P	No. (%)	OR[a]	P	No. (%)	OR[a]	P
KRAS-12	A/A	85 (34)	99 (27)	Ref.		78 (28)	Ref.		21 (26)	Ref.		12 (26)	Ref.		9 (26)	Ref.	
	A/G + G/G	168 (66)	265 (7)	1.4	0.06	205 (72)	1.4	0.09	60 (74)	1.4	0.3	35 (74)	1.3	0.4	25 (74)	1.4	0.4
KRAS-1	A/A	203 (80)	279 (7)	Ref.		224 (79)	Ref.		55 (68)	Ref.		36 (77)	Ref.		19 (56)	Ref.	
	A/C + C/C	50 (20)	85 (23)	1.2	0.4	59 (21)	1.1	0.8	26 (32)	1.8	0.04	11 (23)	1.2	0.7	15 (44)	3.0	0.004
KRAS-6	-/-	163 (64)	217 (60)	Ref.		171 (61)	Ref.		43 (53)	Ref.		29 (62)	Ref.		14 (41)	Ref.	
	-/T + T/T	90 (36)	147 (40)	1.2	0.4	109 (39)	1.1	0.7	38 (47)	1.5	0.1	18 (38)	1.0	0.9	20 (59)	2.4	0.02
CASC1-1	A/A	161 (64)	211 (58)	Ref.		169 (60)	Ref.		42 (52)	Ref.		27 (59)	Ref.		15 (44)	Ref.	
	A/G + G/G	92 (36)	153 (42)	1.2	0.3	114 (40)	1.1	0.6	39 (48)	1.5	0.1	19 (41)	1.2	0.6	19 (56)	2.0	0.06
CASC1-4	Arg/Arg	157 (62)	210 (58)	Ref.		168 (59)	Ref.		42 (52)	Ref.		27 (57)	Ref.		15 (44)	Ref.	
	Arg/Ser + Ser/Ser	96 (38)	154 (42)	1.1	0.4	115 (41)	1.1	0.7	39 (48)	1.4	0.2	20 (43)	1.1	0.7	19 (56)	2.0	0.08
CASC1-5	T/T	157 (62)	207 (57)	Ref.		165 (58)	Ref.		42 (82)	Ref.		26 (55)	Ref.		16 (47)	Ref.	
	T/C + C/C	96 (38)	157 (43)	1.2	0.3	118 (42)	1.1	0.5	9 (18)	1.4	0.2	21 (45)	1.3	0.5	18 (53)	1.7	0.1
LRMP-7	Ser/Ser	172 (68)	231 (63)	Ref.		183 (65)	Ref.		48 (59)	Ref.		31 (66)	Ref.		17 (50)	Ref.	
	Ser/Cys + Cys/Cys	81 (32)	133 (37)	1.2	0.4	100 (35)	1.1	0.6	33 (41)	1.3	0.3	16 (34)	1.0	1.0	17 (50)	1.9	0.09
LRMP-6	Val/Val	201 (79)	288 (79)	Ref.		223 (79)	Ref.		65 (80)	Ref.		37 (79)	Ref.		28 (82)	Ref.	
	Val/Leu + Leu/Leu	52 (21)	76 (21)	1.0	0.9	60 (21)	1.0	1.0	16 (20)	1.0	0.9	10 (21)	1.1	0.8	6 (18)	0.8	0.7
LRMP-4	C/C	91 (36)	139 (38)	Ref.		107 (38)	Ref.		32 (40)	Ref.		18 (38)	Ref.		14 (41)	Ref.	
	C/T + T/T	162 (64)	225 (62)	0.9	0.6	176 (62)	0.9	0.6	49 (60)	0.9	0.7	29 (62)	0.9	0.8	20 (59)	0.8	0.6
LRMP-1	G/G	81 (32)	133 (37)	Ref.		105 (37)	Ref.		28 (35)	Ref.		17 (36)	Ref.		11 (32)	Ref.	
	G/A + A/A	172 (68)	231 (63)	0.8	0.2	178 (63)	0.8	0.2	53 (65)	1.0	0.9	30 (64)	0.9	0.8	23 (68)	1.1	0.9

	Case							
	Small-sized ADC with BAC components			Smoking habit				
				Non-smoker			Smoker		
	No. (%)	OR[a]	P	No. (%)	OR[b]	P	No. (%)	OR[b]	P
KRAS-12	49 (32)	Ref.		44 (25)	Ref.		54 (29)	Ref.	
	103 (68)	1.1	0.8	130 (75)	1.4	0.1	135 (71)	1.3	0.2
KRAS-1	115 (76)	Ref.		135 (77)	Ref.		146 (77)	Ref.	
	37 (24)	1.3	0.3	41 (23)	1.2	0.5	44 (23)	1.2	0.5
KRAS-6	94 (62)	Ref.		106 (61)	Ref.		110 (58)	Ref.	
	58 (38)	1.1	0.6	68 (39)	1.1	0.8	79 (42)	1.3	0.2
CASC1-1	93 (61)	Ref.		104 (60)	Ref.		106 (56)	Ref.	
	59 (39)	1.1	0.7	70 (40)	1.1	0.6	83 (44)	1.3	0.2
CASC1-4	93 (61)	Ref.		102 (59)	Ref.		107 (57)	Ref.	
	59 (39)	1.1	0.8	72 (41)	1.1	0.7	82 (43)	1.2	0.3
CASC1-5	92 (61)	Ref.		100 (57)	Ref.		106 (56)	Ref.	
	60 (39)	1.1	0.7	74 (43)	1.2	0.5	83 (44)	1.2	0.3
LRMP-7	105 (69)	Ref.		109 (63)	Ref.		121 (64)	Ref.	
	47 (31)	1.0	0.8	65 (37)	1.2	0.4	68 (36)	1.2	0.5
LRMP-6	127 (84)	Ref.		138 (79)	Ref.		149 (79)	Ref.	
	25 (16)	0.8	0.4	36 (21)	1.0	0.9	40 (21)	1.0	0.9
LRMP-4	67 (44)	Ref.		75 (43)	Ref.		65 (34)	Ref.	
	85 (56)	0.7	0.2	99 (57)	0.8	0.3	125 (66)	1.1	0.6
LRMP-1	61 (40)	Ref.		70 (40)	Ref.		63 (33)	Ref.	
	91 (60)	0.7	0.2	104 (60)	0.8	0.3	126 (67)	0.9	0.8

[a]Adjusted for gender, age and smoking dosage.
[b]Adjusted for gender and age.

Table IV. Frequency of the *Pst1* haplotypes in cases and controls

Haplotype	Polymorphism						Frequency (95% CI)				
	KRAS-1	KRAS-6	CASC1-1	CASC1-4	CASC1-5	Control	ADC				
							All	AAH absent	AAH present		
									All	1 AAH	≥2 AAHs
1	A	—	A	Arg	T	0.78 (0.75–0.82)	0.75 (0.72–0.78)	0.76 (0.73–0.80)	0.71 (0.64–0.78)	0.76 (0.67–0.84)	0.65 (0.53–0.76)
2	C	T	G	Ser	C	0.10 (0.07–0.12)	0.12 (0.10–0.14)	0.11 (0.08–0.14)	0.15 (0.10–0.21)	0.12 (0.06–0.18)	0.21 (0.11–0.30)
3	A	T	G	Ser	C	0.09 (0.07–0.12)	0.10 (0.07–0.12)	0.10 (0.07–0.12)	0.09 (0.05–0.13)	0.09 (0.03–0.14)	0.09 (0.02–0.15)

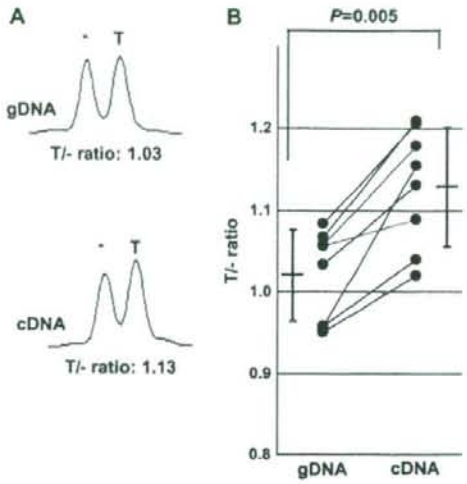

Fig. 2. Differential messenger RNA expression between two polymorphic *KRAS* alleles. (**A**) Electrophoregram for genomic DNA (gDNA) and cDNA of a representative case. Relative amounts of PCR products from the minor (T) allele to those from the major (−) allele are shown below as T/− ratios. (**B**) Relative amounts of PCR products from the minor allele to those from the major allele in genomic DNA and cDNA of non-cancerous lung tissues of eight KRAS-6 hetrozygotes. Mean ± SD for the relative amounts in genomic DNA and cDNA is also indicated with a *P* value by the paired *t*-test.

probably that *Casc1* contributes to lung ADC/adenoma susceptibility by expressing polymorphic proteins with differential activity. This result is in contrast to the case of the *Kras* gene, for which polymorphisms associated with amino acid substitution have not been found, while differential expression between polymorphic alleles was observed (18). Interestingly, the human *CASC1* gene also has a polymorphism with amino acid substitution, CASC-4. Therefore, it is possible that the polymorphism also causes a difference in the activity of CASC1 protein as in the case of mouse Casc1 protein. Thus, the functional significance of *CASC1* SNPs should be further investigated both on expression level and protein activity to clarify the involvement of the *CASC1* gene in ADC/AAH susceptibility, and such a study is in progress in our laboratory.

The present study indicated that *KRAS/Kras* polymorphisms are involved in the susceptibility to lung tumor development by causing differential expression levels of the *KRAS* oncogene, not only in mice but also in humans. Thus, a further study should be done to elucidate molecular mechanisms underlying the differential expression between susceptible and resistant *KRAS/Kras* alleles. In the present study, transcripts from the minor allele for the KRAS-6 polymorphism were shown to be more abundant than those from the major allele. However, it remains unknown whether this polymorphism is responsible for differential expression or not. The KRAS-6 polymorphism is located in a 94 kb LD region covering introns and the 3′-UTR of the *KRAS* gene (Figure 1), and 10 of other polymorphisms have been identified in this region. Notably, the ratios of the *KRAS* transcripts between the major and minor alleles for the KRAS-6 polymorphism were different among the eight cases examined; therefore, it is possible that *KRAS* expression is affected by several polymorphisms. Introns and the 3′-UTR of the *KRAS/Kras* gene contain several genomic segments with significant homologies between humans and mice (http://genome.ucsc.edu/). Thus, it is possible that such segments have common functions in the expression of *KRAS/Kras* gene, and therefore, polymorphisms in these regions are responsible for the differential levels of *KRAS/Kras* gene expression. Notably, genomic fragments of 50 bp in size encompassing the KRAS-1 and -6 polymorphisms, which showed associations with risk for ADC accompanied by multiple AAHs, did not show significant homologies with the

mouse genome. Thus, these two polymorphisms are unlikely to be responsible ones. Further functional and genetic studies on *KRAS* will give us more critical information on the involvement of *KRAS* in lung tumorigenesis in humans.

Supplementary material

Supplementary Figure 1 can be found at http://carcin.oxfordjournals.org/

Funding

Ministry of Health, Labor and Welfare for Research on Human Genome Tailor-made and for Cancer Research (16S-1).

Acknowledgements

We thank Dr Koji Tsuta of the National Cancer Center Hospital for help in pathological examination. We thank Ms Sachiyo Mimaki, Kaoru Toyama and Rumi Ono for technical assistance.

Conflict of Interest Statement: None declared.

References

1. Parkin,M. *et al.* (2004) Lung cancer epidemiology and etiology. In Travis,W.D., Brambilla,E., Muller-Hermelink,H.K. and Harris,C.C. (eds) World Health Organization Classification of Tumors: Pathology and Genetics, Tumours of Lung, Pleura, Thymus and Heart. IARC Press, Lyon, pp. 31–34.
2. Colvy,T. *et al.* (2004) Adenocarcinoma. In Travis,W.D., Brambilla,E., Muller-Hermelink,H.K. and Harris,C.C. (eds) World Health Organization Classification of Tumors: Pathology and Genetics, Tumours of Lung, Pleura, Thymus and Heart. IARC Press, Lyon, pp. 35–44.
3. Nakachi,K. *et al.* (1995) Association of cigarette smoking and CYP1A1 polymorphisms with adenocarcinoma of the lung by grades of differentiation. *Carcinogenesis*, **16**, 2209–2213.
4. Sunaga,N. *et al.* (2002) Contribution of the NQO1 and GSTT1 polymorphisms to lung adenocarcinoma susceptibility. *Cancer Epidemiol. Biomarkers Prev.*, **11**, 730–738.
5. Larsen,J.E. *et al.* (2006) CYP1A1 Ile462Val and MPO G-463A interact to increase risk of adenocarcinoma but not squamous cell carcinoma of the lung. *Carcinogenesis*, **27**, 525–532.
6. Kohno,T. *et al.* (2006) Association of the OGG1-Ser326Cys polymorphism with lung adenocarcinoma risk. *Cancer Sci.*, **97**, 724–728.
7. Malkinson,A.M. (1989) The genetic basis of susceptibility to lung tumors in mice. *Toxicology*, **54**, 241–271.
8. Gariboldi,M. *et al.* (1993) A major susceptibility locus to murine lung carcinogenesis maps on chromosome 6. *Nat. Genet.*, **3**, 132–136.
9. Fijneman,R.J. *et al.* (1996) Complex interactions of new quantitative trait loci, Sluc1, Sluc2, Sluc3, and Sluc4, that influence the susceptibility to lung cancer in the mouse. *Nat. Genet.*, **14**, 465–467.
10. Manenti,G. *et al.* (1996) Genetic mapping of a pulmonary adenoma resistance (Par1) in mouse. *Nat. Genet.*, **12**, 455–457.
11. Manenti,G. *et al.* (2003) Outbred CD-1 mice carry the susceptibility allele at the pulmonary adenoma susceptibility 1 (Pas1) locus. *Carcinogenesis*, **24**, 1143–1148.
12. Balmain,A. *et al.* (1998) Cancer resistance genes in mice: models for the study of tumour modifiers. *Trends Genet.*, **14**, 139–144.
13. Sakiyama,T. *et al.* (2005) Association of amino acid substitution polymorphisms in DNA repair genes TP53, POLI, REV1 and LIG4 with lung cancer risk. *Int. J. Cancer*, **114**, 730–737.
14. Maria,D.A. *et al.* (2003) Pulmonary adenoma susceptibility 1 (Pas1) locus affects inflammatory response. *Oncogene*, **22**, 426–432.
15. Zhang,Z. *et al.* (2003) Positional cloning of the major quantitative tra locus underlying lung tumor susceptibility in mice. *Proc. Natl Acad. Sc USA*, **100**, 12642–12647.
16. Manenti,G. *et al.* (2004) Haplotype sharing suggests that a genomic seg ment containing six genes accounts for the pulmonary adenoma suscept bility 1 (Pas1) locus activity in mice. *Oncogene*, **23**, 4495–4504.
17. Liu,P. *et al.* (2006) Candidate lung tumor susceptibility genes identifie through whole-genome association analyses in inbred mice. *Nat. Genet* **38**, 888–895.
18. To,M.D. *et al.* (2006) A functional switch from lung cancer resistance t susceptibility at the Pas1 locus in Kras2LA2 mice. *Nat. Genet.*, **3** 926–930.
19. Manenti,G. *et al.* (1997) Association of chromosome 12p genetic poly morphisms with lung adenocarcinoma risk and prognosis. *Carcinogenesi* **18**, 1917–1920.
20. Dragani,T.A. *et al.* (2000) Population-based mapping of pulmonary ad noma susceptibility 1 locus. *Cancer Res.*, **60**, 5017–5020.
21. Manenti,G. *et al.* (2000) Predisposition to lung tumorigenesis. *Toxico Lett.*, **112-113**, 257–263.
22. Manenti,G. *et al.* (2006) A V141L polymorphism of the human LRMP gen is associated with survival of lung cancer patients. *Carcinogenesis*, **2** 1386–1390.
23. Niho,S. *et al.* (1999) Monoclonality of atypical adenomatous hyperplasia o the lung. *Am. J. Pathol.*, **154**, 249–254.
24. Kerr,K.M. *et al.* (2004) Atypical adenomatous hyperplasia. In Travis,W.D Brambilla,E., Muller-Hermelink,H.K. and Harris,C.C. (eds) World Healt Organization Classification of Tumors: Pathology and Genetics, Tumou of Lung, Pleura, Thymus and Heart. IARC Press, Lyon, pp. 73–75.
25. Koga,T. *et al.* (2002) Lung adenocarcinoma with bronchioloalveolar carc noma component is frequently associated with foci of high-grade atypic adenomatous hyperplasia. *Am. J. Clin. Pathol.*, **117**, 464–470.
26. Sterner,D.J. *et al.* (1997) Prevalence of pulmonary atypical alveolar ce hyperplasia in an autopsy population: a study of 100 cases. *Mod. Pathol* **10**, 469–473.
27. Yokose,T. *et al.* (2000) High prevalence of atypical adenomatous hyperpl sia of the lung in autopsy specimens from elderly patients with malignar neoplasms. *Lung Cancer*, **29**, 125–130.
28. Yokose,T. *et al.* (2001) Atypical adenomatous hyperplasia of the lung i autopsy cases. *Lung Cancer*, **33**, 155–161.
29. Brambilla,E. *et al.* (2001) The new World Health Organization classific tion of lung tumours. *Eur. Respir. J.*, **18**, 1059–1068.
30. Travis,W., Colby,T.V., Corrin,B., Shimosato,Y. and Brambilla,E. (eds) 199 Histological Typing of Lung and Pleural Tumors. Springer-Verla Heidelberg, Germany.
31. Breslow,N.E. *et al.* (1980) Statistical methods in cancer research. Volum I—The analysis of case-control studies. *IARC Sci. Publ.*, **32**, 5–338.
32. Karasaki,H. *et al.* (1997) Roles of the Pas1 and Par2 genes in determinatio of the unique, intermediate susceptibility of BALB/cByJ mice to urethan induction of lung carcinogenesis: differential effects on tumor multiplicit size and Kras2 mutations. *Oncogene*, **15**, 1833–1840.
33. Lin,L. *et al.* (1998) Additional evidence that the K-ras protooncogene i a candidate for the major mouse pulmonary adenoma susceptibility (Pas-1 gene. *Exp. Lung Res.*, **24**, 481–497.
34. Shigematsu,H. *et al.* (2006) Somatic mutations of epidermal growth fac tor receptor signaling pathway in lung cancers. *Int. J. Cancer*, **11** 257–262.
35. Westra,W.H. *et al.* (1996) K-ras oncogene activation in atypical alveol hyperplasias of the human lung. *Cancer Res.*, **56**, 2224–2228.
36. Manenti,G. *et al.* (1998) Genetic mapping of cancer susceptibility/resi tance loci in the mouse. *Recent Results Cancer Res.*, **154**, 292–297.
37. Wang,M. *et al.* (2003) Fine mapping and identification of candidate pu monary adenoma susceptibility 1 genes using advanced intercross line *Cancer Res.*, **63**, 3317–3324.

Received October 14, 2007; revised January 16, 2008; accepted February 7, 2008

Association of p16 Homozygous Deletions with Clinicopathologic Characteristics and EGFR/KRAS/p53 Mutations in Lung Adenocarcinoma

Reika Iwakawa,[1,6] Takashi Kohno,[1] Yoichi Anami,[4] Masayuki Noguchi,[4] Kenji Suzuki,[2] Yoshihiro Matsuno,[3] Kazuhiko Mishima,[5] Ryo Nishikawa,[5] Fumio Tashiro,[6] and Jun Yokota[1]

Abstract **Purpose:** The *p16* gene is frequently inactivated in lung adenocarcinoma. In particular, homozygous deletions (HD) have been frequently detected in cell lines; however, their frequency and specificity is not well-established in primary tumors. The purpose of this study was to elucidate the prevalence and the timing for the occurrence of p16 HDs in lung adenocarcinoma progression *in vivo*.

Experimental Design: Multiple ligation-dependent probe amplification was used for the detection of p16 HDs in 28 primary small-sized lung adenocarcinomas and 22 metastatic lung adenocarcinomas to the brain. Cancer cells were isolated from primary adenocarcinoma specimens by laser capture microdissection. HDs were confirmed by quantitative real-time genomic PCR analysis.

Results: HDs were detected in 8 of 28 (29%) primary tumors, including 2 of 8 (25%) noninvasive bronchioloalveolar carcinomas, and 5 of 22 (26%) brain metastases, respectively. No significant associations were observed between p16 HDs and gender, age, smoking history, stage, and prognosis. HDs were detected with similar frequencies (17–29%) among adenocarcinomas with epidermal growth factor receptor (EGFR) mutations, with KRAS mutations, and without EGFR/KRAS mutations, and with similar frequencies (22–28%) between adenocarcinomas with and without p53 mutations.

Conclusions: p16 HDs occur early in the development of lung adenocarcinomas and with similar frequencies among EGFR type, KRAS type, and non-EGFR/KRAS type lung adenocarcinomas. Tobacco carcinogens would not be a major factor inducing p16 HDs in lung adenocarcinoma progression.

Adenocarcinoma is the most common histologic type of lung cancer. Recent molecular analyses have indicated that lung adenocarcinoma can be divided into at least three types; the epidermal growth factor receptor (EGFR) type, the KRAS type, and the non-EGFR/KRAS type, based on accumulated genetic alterations in adenocarcinoma cells (1, 2). The *p16* tumor suppressor gene is frequently inactivated in lung adenocarcinomas, most prominently through promoter methylation and homozygous deletion (HD), and less frequently through intragenic mutation (3–6). In particular, p16 methylation is known to occur in close association with tobacco carcinogen exposure and preferentially in the KRAS type adenocarcinomas (1). Molecular analyses of small-sized adenocarcinomas revealed that p16 methylation occurs in the course of progression from noninvasive bronchioloalveolar carcinomas (BAC) to invasive ones, and its occurrence is associated with smoking history, staging, and prognosis (7). However, it is still unknown whether p16 HD also occurs preferentially in the KRAS type or not. In addition, the involvement of tobacco smoking in the occurrence of p16 HD is also unclear because both positive and negative associations between tobacco smoking and HD have been reported (5, 6). Indeed, p16 HDs have been reported to occur with a highly variable frequency in primary lung adenocarcinomas (0–40%; refs. 3–6, 8). HD can be easily masked if a large fraction of noncancerous cells are contaminated in tumor tissues, in particular, in the analysis of small tumors with a BAC component. Thus, such an inconsistency could come not only from the diversity and/or heterogeneity of lung adenocarcinomas but also from tumor tissues used for the analysis and also from the methods used for the detection of HDs. For instance, immunohistochemical analyses of p16 proteins have shown that a considerable

Authors' Affiliations: [1]Biology Division, National Cancer Center Research Institute, [2]Thoracic Surgery Division and [3]Diagnostic Pathology Division, National Cancer Center Hospital, Tokyo, Japan; [4]Department of Pathology, Institute of Basic Medical Sciences, Graduate School of Comprehensive Human Sciences, Tsukuba University, Ibaraki, Japan; [5]Department of Neuro-Oncology, Comprehensive Cancer Center, International Medical Center, Saitama Medical University, Saitama, Japan; and [6]Department of Biological Science and Technology, Faculty of Industrial Science and Technology, Tokyo University of Science, Chiba, Japan

Received 10/5/07; revised 2/24/08; accepted 2/28/08.

Grant support: Grants-in-Aid from the Ministry of Health, Labor and Welfare for the Third-Term Comprehensive 10-Year Strategy for Cancer Control and for Cancer Research (16-1) and a Grant-in-Aid for the Program for Promotion of Fundamental Studies in Health Sciences of the National Institute of Biomedical Innovation (NiBio).

The costs of publication of this article were defrayed in part by the payment of page charges. This article must therefore be hereby marked *advertisement* in accordance with 18 U.S.C. Section 1734 solely to indicate this fact.

Requests for reprints: Jun Yokota, Biology Division, National Cancer Center Research Institute, 1-1, Tsukiji 5-chome, Chuo-ku, Tokyo 104-0045, Japan. Phone: 81-33547-5272; Fax: 81-33542-0807; E-mail: jyokota@ncc.go.jp.

doi:10.1158/1078-0432.CCR-07-4552

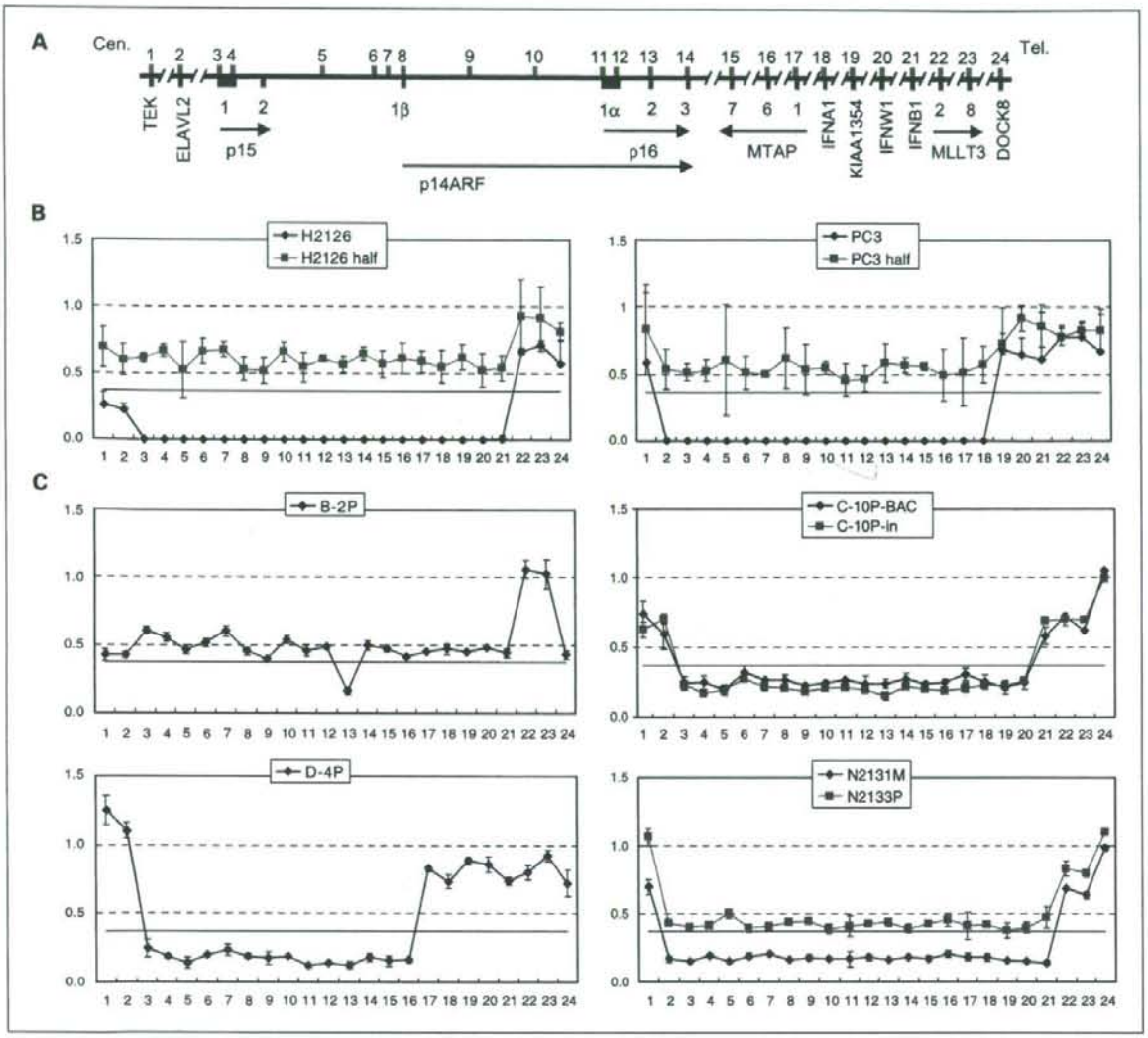

Fig. 1. HDs of the *p16* gene detected by MLPA analysis. *A*, physical map of the chromosome 9p region. Top, positions of 24 probes from nos. 1 to 24 (*red*) in the order from centromere (*Cen.*) to telomere (*Tel.*). Bottom, positions of 12 genes in this region (*light blue*). Exons (*numbers*) and orientations (*arrows*) of the *p15*, *p14ARF*, *p16*, *MTAP*, and *MLLT3* genes. *B*, definition of p16 HDs by MLPA analysis. Relative copy numbers of the 24 loci in two lung adenocarcinoma cell lines, H2126 and PC3 (*blue dots/lines*), and those in mixed samples of the same amounts of DNA from these cell lines and normal lung tissue (*pink dots/lines*; H2126 half and PC3 half, respectively). *C*, results of MLPA analysis for cases B-2P, C-10P, D-4P, and N2131M/N2133P showing HDs of the *p16* gene. As for case C-10P, both the BAC component (*BAC; blue dots/lines*) and the invasive region (*in; pink dots/lines*) of the tumor were analyzed. N2131M (*blue*) and N2133P (*pink*) are a brain metastasis and the primary tumor from the same patient, respectively.

fraction of adenocarcinomas are negative for p16 protein expression without clear evidence of an inactivating event by molecular analyses of the *p16* gene (4, 5, 7). Thus, it has been assumed that p16 HD is a causative event for the absence of p16 protein in these adenocarcinoma cases. However, due to the lack of comprehensive analysis for p16 HDs, the prevalence, specificity, and the timing for the occurrence of p16 HDs in lung adenocarcinoma progression *in vivo* is still unclear.

In this study, we investigated the association of p16 HDs with clinicopathologic characteristics, including smoking history, of lung adenocarcinomas and with the status of EGFR, KRAS, and p53 mutations in lung adenocarcinomas. To obtain more critical information than previous studies for the timing of its occurrence in the progression of lung adenocarcinomas, we analyzed two typical stages of lung adenocarcinomas. One is a primary small-sized adenocarcinoma of ≤2 cm in maximum diameter as a representative of early stage lung adenocarcinomas, and the other is a brain metastasis as a representative of late stage lung adenocarcinomas. To exclude the possible overlooking of HDs in the analysis due to contamination of noncancerous cells in tumor tissues, a laser capture

microdissection method was applied for the isolation of cancer cells from small-sized primary lung adenocarcinomas. Brain metastases are known to be relatively solid and generally contain a small amount of noncancerous cells in tumor tissues; therefore, macrodissected samples were used for the analysis. Recently, a simple and effective method, which is called multiplex ligation-dependent probe amplification (MLPA), to measure the copy number of up to 45 genomic loci in a single experiment, was developed and has been applied for the detection of large deletions in/of various genes in the human genome DNA sequence (9). For instance, this method was successfully applied for the detection of p16 hemizygous deletions in melanoma families (10) and p16 HDs in head and neck squamous cell carcinoma cell lines (11). Thus, we applied this method for the detection of p16 HDs in surgically resected lung adenocarcinomas. HDs were detected with similar frequencies of 23% to 40% in lung adenocarcinomas of any progression stage—from noninvasive carcinomas to advanced ones. The deletions were also detected with similar frequencies among EGFR type, KRAS type, and non-EGFR/KRAS type adenocarcinomas, and were not associated with tobacco smoking and poor prognosis.

Materials and Methods

Patients and tissues. Twenty-eight primary small-sized (≤2 cm in maximum diameter) adenocarcinomas, 22 brain metastases, and corresponding noncancerous tissues were obtained at surgery from lung adenocarcinoma patients treated at the National Cancer Center Hospital, Tokyo and at the Saitama Medical University. In 4 of the 22 brain metastasis cases, the corresponding primary tumors were also obtained at surgery. The surgically resected specimens were fixed routinely with 10% formalin and embedded in paraffin for histologic examination. All the sections were stained with H&E and examined by light microscopy. The tumors were pathologically diagnosed according to the tumor-node-metastasis classification of malignant tumors (12). The primary small-sized adenocarcinomas were further classified into three types according to the histologic classification of small-sized adenocarcinoma of the lung reported by Noguchi and colleagues (13), and there were 8 type B, 15 type C, and 5 type D adenocarcinomas. These 28 tumors and corresponding noncancerous tissues were fixed with methanol and embedded in paraffin. Cancer cells were then microdissected using the Pixcell Laser Capture Microdissection system (Arcturus Engineering), and their genomic DNAs were extracted as described previously (14). Representative figures of type B and C tumors before and after microdissection have been shown in our previous article (14). All of the 22 brain metastases, corresponding primary tumors, and noncancerous tissues were macrodissected and stored at -80°C until DNA extraction. Genomic DNAs were prepared as previously described (15).

Cell lines. Three lung adenocarcinoma cell lines, H2126, A549, and PC3, were used as positive controls of p16 HDs in MLPA and quantitative real-time genomic PCR (QRT-G-PCR) analysis. Genomic DNA were prepared as previously described (15). Incidence as well as regions of p16 HDs in 55 lung adenocarcinoma cell lines, including these three cell lines, were determined by multiplex PCR analysis in our previous studies (3).

MLPA analysis. MLPA was carried out using the P024B kit for the 9p21 CDKN2A/2B region (MRC-Holland) according to the manufacturer's protocol. The kit contains 12 probes covering the *p15/p14ARF/p16* genes, 12 probes for 9 other genes on chromosome 9p, and 15 control probes for nonchromosome 9p loci. Genes on chromosome 9p included in this screen were *TEK, ELAVL2, CDKN2B (p15), CDKN2A (p14ARF/p16), MTAP, IFNA1, KIAA1354, IFNW1, IFNB1, MLLT3,* and *DOCK8 (FLJ00026)* in the order from centromere to telomere (Fig. 1A). Experiments were done in a half volume until the ligation reaction step, and then by the supplied protocol. Briefly, 12.5 to 50 ng of genomic DNA in 2.5 to 5 μL of TE buffer were heat-denatured and hybridized to probes for 16 h at 60°C. The hybridized probes were then ligated and amplified by PCR of 35 cycles at 60°C for 30 s and 72°C for 60 s. PCR products were separated by capillary electrophoresis using the ABI3700 Automated Capillary DNA Sequencer with a 50-cm capillary array, ABI POP-6 polymer, and GeneScan-ROX 500 size standards (Applied Biosystems). Analysis was automated using ABI PRISM GeneScan Analysis software version 3.7, and Genotyper Analysis software version 3.7 (Applied Biosystems). PCR and electrophoresis, respectively, were done in duplicate, and the mean of four values was calculated and considered to be the DNA copy number ratio of each locus.

Data analysis. The relative DNA copy number of each locus was calculated as follows. First, the value for the sum of 15 autosomal control probe peak areas in a lung adenocarcinoma sample was adjusted to the mean value for those in two or three normal lung tissue samples in the same run. Each of the 39 probe peak areas was then divided by the sum of the peak areas of the 15 autosomal control probe peak areas. Finally, the relative DNA copy number ratio of each of the 39 chromosome loci in the lung adenocarcinoma samples against the normal lung tissue samples was calculated. Theoretically, ratios close to 1.0 indicated that two DNA copies were present (i.e., wild-type), a ratio of 0.5 indicated that one copy was absent (i.e., hemizygous deletion), and a ratio of 0.0 indicated that both copies were absent (i.e., homozygous deletion). The criteria for hemizygous deletions and HDs of the 39 loci by MLPA analysis were defined using MLPA data from three lung adenocarcinoma cell lines with p16 HDs as described in Results and Discussion. The *p16* gene was then defined as homozygously deleted or not in each sample. Because the purpose of this study is to evaluate the prevalence of p16 HD, hemizygous deletions were not evaluated from MLPA data.

QRT-G-PCR analysis. TaqMan-MGB probes and primers were designed using Primer Express software (Applied Biosystems) and were optimized according to the manufacturer's guidelines. Target and reference locus probes were labeled with FAM and VIC, respectively. Probe sequences were as follows: no. 9, 5′-AACTCCTCCACTGATTAC-3′; and 2p14, 5′-CCAGCCTATTCCTGC-3′. Primer sequences were as follows: no. 9-F/R, 5′-GGGTCTCCTTCATTTGGTGAAA-3′/5′-GGATCCCAGGGAGGAGAGTCT-3′; and 2p14-F/R, 5′-AAGAAGACTGGAGTGGTGTTTGG-3′/5′-CACAATGCTGAATACTGTCAATGAAA-3′. PCR was carried out in duplicate using 1 ng of DNA as a template. Primer and probe concentrations were optimized for each target according to the manufacturer's instructions. The PCR program consisted of 50°C for 2 min and 95°C for 15 min followed by 45 cycles of 95°C for 15 s and 60°C for 1 min. Standard curves for the copy numbers of the target and reference genes were generated using serially diluted (0.04–25 ng) normal lung tissue DNA. Data analysis was carried out using ABI Prism 7900HT Sequence Detection Software. DNA copy number ratios were calculated as the average copy number of the target locus divided by the average copy number of the reference locus, and then normalized against the normal lung tissue DNA to give a normalized DNA copy number ratio.

Immunohistochemistry. Immunohistochemical analysis of p16 protein was performed as described previously (7) using 4-μm sections cut from methanol-fixed and paraffin-embedded specimens of 28 primary small-sized adenocarcinomas, which were subjected to MLPA analysis. Positivity for p16 staining was scored by the same criteria as previously described (7). In brief, only nuclear staining was scored, and was considered to be positive when it was more intense than the background cytoplasmic staining. If <10% of tumor cells displayed p16 protein staining, it was judged negative; and if >10% of them showed strong staining, it was judged positive.

Mutation analysis of the* EGFR, KRAS, *and* p53 *genes. Thirteen of the 28 primary tumors, and 16 of the 22 brain metastases were

Table 1. Frequencies of p16 HDs and EGFR/KRAS/p53 mutations in lung adenocarcinoma

Sample	Subtype	Frequency (%)			
		p16	EGFR	KRAS	p53
Surgical specimen		13/50 (26)	34/50 (68)	4/50 (8)	32/50 (64)
Primary tumor		8/28 (29)	21/28 (75)	2/28 (7)	16/28 (57)
	Type B	2/8 (25)	8/8 (100)	0/8 (0)	2/8 (25)
	Type C	4/15 (27)	12/15 (80)	1/15 (7)	9/15 (60)
	Type D	2/5 (40)	1/5 (20)	1/5 (20)	5/5 (100)
Brain metastasis		5/22 (23)	13/22 (59)	2/22 (9)	16/22 (73)
Cell line*		20/55 (36)	-	-	-

*Defined in our previous study (17).

previously examined for mutations of exons 18 to 21 in the *EGFR* gene, of exons 1 and 2 in the *KRAS* gene, and of exons 4 to 8 in the *p53* gene by genomic PCR and direct sequencing (14, 16). The remaining 15 primary tumors and 6 brain metastases were also examined for these mutations in this study using the same methods.

Statistical analysis. Fisher's exact test was used to assess the association of p16 HDs with clinicopathologic characteristics or mutations of the *EGFR*, *KRAS*, and *p53* genes. $P < 0.05$ was considered to be statistically significant.

Results and Discussion

Detection of HDs by MLPA analysis. We previously determined regions of p16 HDs in various lung cancer cell lines by multiplex genomic PCR analysis (3, 17). Thus, we first validated the sensitivity and specificity of the MLPA method to detect p16 HDs using several lung adenocarcinoma cell lines. No PCR amplification was observed for probes that hybridized to the sequences of HD regions in all the cell lines examined. Representative results of MLPA analysis for two cell lines, H2126 and PC3, are shown in Fig. 1B. We then applied MLPA analysis for the detection of p16 HDs in surgically resected adenocarcinoma samples. Cancer cells of small-sized primary adenocarcinomas were isolated by laser capture microdissection, and brain metastases generally contain a small fraction of noncancerous cells. However, a complete absence of PCR products was not observed for these samples at any chromosomal loci by MLPA analysis. Therefore, we next defined the criteria for p16 HDs by MLPA analysis for surgically resected samples. For this purpose, DNA samples with virtual hemizygous deletions were prepared by mixing the same amounts of DNA from normal lung tissue and from three lung cancer cell lines with p16 HDs, H2126, A549, and PC3. In total, 64 probe loci were homozygously deleted in these cell lines. The mean ± 3 SD of relative DNA copy number ratios for the 64 probe loci in the HD regions among these mixed samples was 0.54 ± 0.17; thus, the range of virtual hemizygous deletions was 0.37 to 0.71. Indeed, none of the 64 probe loci in the HD regions of the mixed samples showed a DNA copy number ratio of >0.71 or <0.37 (Fig. 1B). Therefore, if the DNA copy number ratio for a locus was <0.37, the locus was judged as homozygously deleted in surgically resected lung adenocarcinoma samples.

Under this criterion, one or more loci in the *p15/p14ARF/p16* gene region were judged as homozygously deleted in 8 of 28 primary tumors and in 5 of 22 brain metastases (Table 1). Representative adenocarcinoma cases judged as having HDs of this region by MLPA analysis are shown in Fig. 1C. Case B-2P showed a HD of only one locus (probe no. 13) in exon 2 of the *p16* gene. On the other hand, most of the other 12 cases showed HDs of several genes, including the *p14ARF* and/or *p16* genes (Table 2). Both the invasive region (C-10P-in) and the BAC component (C-10P-BAC) of case C-10P showed HDs of the same loci from *p15* exon 1 to *IFNW1*. In case D-4P, the *p15*, *p14ARF*, *p16*, and *MTAP* genes were homozygously deleted. A metastasis to the brain, case N2131M, showed a large HD of the region from the *ELAVL2* gene to the *IFNB1* gene including the *p16* gene. Furthermore, the relative DNA copy number ratios of the corresponding loci were also decreased in the corresponding primary tumor, N2133P, although the ratios were underrepresented as HDs. This may be attributed to a

Table 2. Regions of p16 HDs on chromosome 9p defined by MLPA analysis

No.	Case		Probe no.																						
	Primary tumor	Brain metastasis	1	2	3	4	5	6	7	8	9	10	11	12	13	14	15	16	17	18	19	20	21	22	23	24
1	B-2P		-	-	-	-	-	-	-	-	-	-	-	-	+	-	-	-	-	-	-	-	-	-	-	-
2	B-8P		-	+	-	+	+	+	-	+	+	-	+	+	+	+	+	+	-	-	-	-	-	-	-	-
3	C-5P		-	-	+	+	+	+	+	+	+	+	+	+	+	+	+	+	+	+	+	+	+	+	+	-
4	C-8P		-	+	+	+	+	+	+	+	+	+	+	+	+	+	+	+	+	+	+	+	+	+	+	-
5	C-10P		-	-	+	+	+	+	+	+	+	+	+	+	+	+	+	+	+	+	+	+	-	-	-	-
6	C-65P		-	-	+	+	+	+	+	+	+	-	+	+	+	+	+	+	+	+	+	-	-	-	-	-
7	D-4P		-	-	+	+	+	+	+	+	+	+	+	+	+	+	+	+	-	-	-	-	-	-	-	-
8	D-12P		-	+	+	+	+	+	+	+	+	+	+	+	+	+	+	+	+	+	+	+	+	-	-	-
9		N181M	-	-	+	+	+	+	+	+	+	+	+	+	+	+	+	+	-	-	-	-	-	-	-	-
10		N571M	-	-	+	+	+	+	+	+	+	+	+	+	+	+	+	+	-	-	-	-	-	-	-	-
11	N2133P	N2131M	-	+	+	+	+	+	+	+	+	+	+	+	+	+	+	+	+	+	+	+	+	-	-	-
12		N2151M	-	-	+	+	+	+	+	+	+	+	+	+	+	+	+	+	+	+	+	+	+	+	-	-
13		N2191M	-	+	+	+	+	+	+	+	+	-	-	-	-	-	-	-	-	-	-	-	-	-	-	-

NOTE: Loci with copy number ratios <0.37 are indicated by (+) and those >0.37 are indicated by (-).

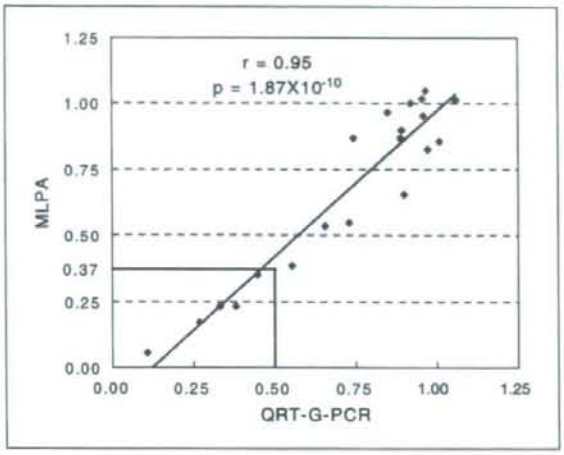

Fig. 2. Correlation between the results of MLPA analysis and those of QRT-G-PCR analysis. Relative DNA copy numbers of the probe no. 9 locus in Fig. 1A on chromosome 9 against the control locus on chromosome 2 defined by the QRT-G-PCR (*X*-axis) and MLPA analyses (*Y*-axis). Sixteen brain metastases and four of the corresponding primary tumors were analyzed. Values <0.5 by QRT-G-PCR analysis and values <0.37 by MLPA analysis (indicated by lines) were considered as having HDs.

contamination of noncancerous cells in the primary tumor sample because this sample was macrodissected but not microdissected. There was no probe loci deleted in all the cases, but six loci (probe nos. 4, 5, 6, 8, 9, and 13) were deleted in 12 of 13 cases, including exon 2 of the *p16* gene (Table 2).

Confirmation of HDs by QRT-G-PCR analysis. QRT-G-PCR was performed to confirm p16 HDs detected by MLPA analysis. Among 15 control probes for nonchromosome 9p loci, a probe for a chromosome 2p14 locus showed the most consistent DNA copy number ratios of nearly 1.0 in surgically resected adenocarcinoma samples. Thus, two primer sets were designed for QRT-G-PCR analysis. One was for the amplification of an MLPA probe locus between the *p14ARF* gene and the *p16* gene (probe no. 9 in Fig. 1A, and hereinafter referred to as the *p14ARF/p16* locus), and the other was for the amplification of a control probe locus on chromosome 2p14.

QRT-G-PCR was carried out for 16 brain metastases and the corresponding 4 primary tumors. Among them, five brain metastases were judged as having HDs of the *p14ARF/p16* locus by MLPA analysis. DNA from normal lung tissue was used as a negative control, and DNA from two lung cancer cell lines with p16 HDs, A549 and H2126, were used as positive controls. No PCR products were detected for the *p14ARF/p16* locus in the A549 and H2126 cell lines (data not shown). The DNA copy number ratios of the *p14ARF/p16* locus in all five cases that had been determined to have HDs of this locus by MLPA analysis were <0.45. Thus, these five cases were also judged as having less than one copy of the *p14ARF/p16* gene by QRT-G-PCR analysis. We further analyzed the association between the results of MLPA analysis and those of QRT-G-PCR analysis among all the 20 cases. The correlation coefficient was 0.95, and a highly significant correlation was observed between them ($P = 1.87 \times 10^{-10}$; Fig. 2). This result gave the agreement for the appropriateness of the criterion for p16 HDs in MLPA analysis.

Occurrence of p16 HDs in early stage lung adenocarcinoma. Based on the results of MLPA analysis, together with the confirmation by QRT-G-PCR analysis, we concluded that p16 HDs were present in 8 of 28 (29%) small-sized primary tumors and in 5 of 22 (23%) brain metastases (Table 1). Among four pairs of brain metastases and the corresponding primary tumors, only one metastasis (N2131M) was judged as having a p16 HD as described above and shown in Fig. 1C, and none of the remaining three cases showed HD in either brain metastases or primary tumors. Small-sized adenocarcinomas

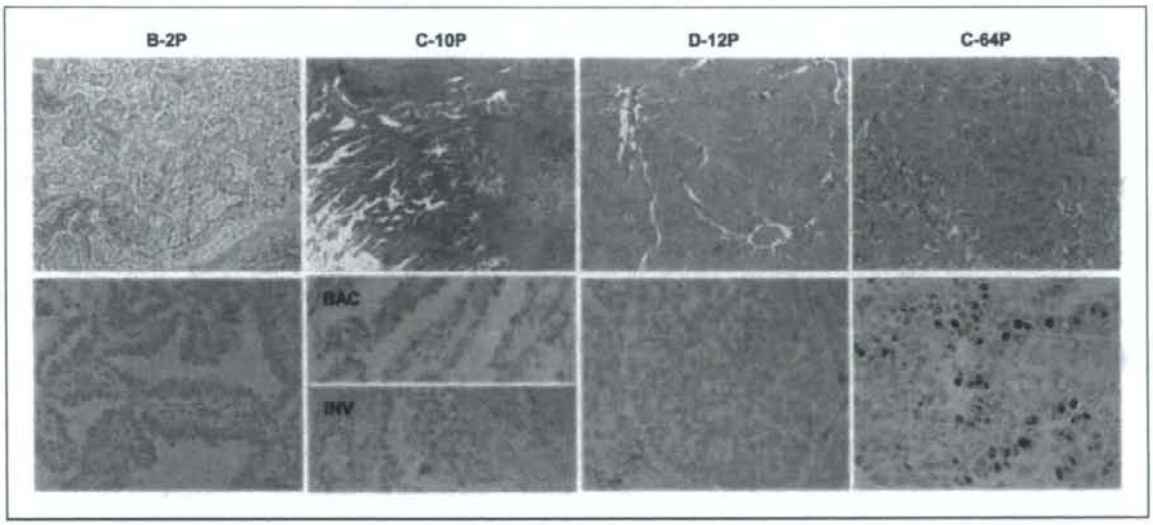

Fig. 3. Histology (H&E; original magnification, ×100 for B-2P/C-12P/C-64P and ×40 for C-10P; *top*) of small-sized lung adenocarcinomas and immunohistochemical staining of p16 protein (original magnification, ×400; *bottom*) in the corresponding tissues. B-2P, C-10P, and D-12P are representative cases of type B, C, and D tumors with p16-negative staining, and C-64P is a representative case of type C tumors with p16-positive staining. A BAC component (*BAC*) and an invasive region (*INV*) are shown separately for C-10P.

Table 3. Associations of p16 HDs with p16 protein expression, clinicopathologic characteristics, and EGFR/KRAS/p53 mutations in lung adenocarcinoma

Clinicopathologic characteristic and genotype	Subset	No. of cases	p16 HD (%)				P*
			+	-			
p16 protein expression †	+	13	0 (0)	13 (100)			<0.01
	-	15	8 (53)	7 (47)			
Gender	Male	30	7 (23)	23 (77)			0.74
	Female	20	6 (30)	14 (70)			
Age	<59	25	8 (32)	17 (68)			0.52
	≧59	25	5 (20)	20 (80)			
Smoking history	Smoker	28	7 (25)	21 (75)			>0.99
	Nonsmoker	22	6 (27)	16 (73)			
Pathologic stage †	I	16	5 (31)	11 (69)			>0.99
	II-III	12	3 (25)	9 (75)			
5-year survival †	+	19	4 (21)	15 (79)			0.37
	-	9	4 (44)	5 (56)			
EGFR/KRAS ‡	E(+)/K(-)	34	10 (29)	24 (71)	]>0.99	]>0.99	0.47
	E(-)/K(+)	4	1 (25)	3 (75)			
	E(-)/K(-)	12	2 (17)	10 (83)			
p53	Mutation(+)	32	9 (28)	23 (72)			0.75
	Mutation(-)	18	4 (22)	14 (78)			

*Fisher's exact test.
† Defined for 28 patients with primary lung adenocarcinoma.
‡ E(+), EGFR mutation(+); E(-), EGFR mutation(-); K(+), KRAS mutation(+); K(-), KRAS mutation(-).

were further classified histologically into types B, C, and D (Fig. 3). Type B tumors are noninvasive BACs and type C tumors are invasive adenocarcinomas with noninvasive BAC components. p16 HDs were detected in 2 of 8 (25%) type B tumors and in 4 of 15 (27%) type C tumors, in particular, in BAC components of two type C tumors (cases C-10P and C-65P). Type D tumors are invasive, poorly differentiated adenocarcinomas and p16 HDs were detected in 2 of 5 (40%) of the type D tumors. Thus, p16 HDs were present with similar frequencies of 25% to 40% in noninvasive and invasive primary adenocarcinomas. We previously reported that p16 HDs were present in 20 of 55 (36%) lung adenocarcinoma cell lines (17). Thus, the frequency of p16 HDs in small-sized primary adenocarcinomas was not significantly lower than, but similar to, those in brain metastases and cultured cell lines. These results strongly indicate that most p16 HDs detected in the cell lines occurred *in vivo* during adenocarcinoma progression and were retained during cultivation *in vitro* of adenocarcinoma cell lines. Similar frequencies of p16 HDs between noninvasive and invasive adenocarcinomas and between primary and metastatic adenocarcinomas further indicate that p16 HD occurs early in the multistage carcinogenic process of lung adenocarcinomas.

No p16 expression in tumors with p16 HDs. Because one of the purposes of this study was to confirm the immunohistochemical negativity of adenocarcinoma cells with p16 HDs, we further performed an immunohistochemical analysis on 28 cases of small-sized adenocarcinomas, all of which were subjected to MLPA analysis. Fifteen of the 28 cases (54%) showed negative immunoreactivity for p16 protein. As predicted, all eight cases with p16 HDs following MLPA analysis were negative for p16 protein expression (Table 3). Representative results of immunohistochemical staining for type B, C, and D tumors are shown in Fig. 3. It was noted that most tumor cells were clearly negative for nuclear p16 staining in these eight cases, and that both BAC components and invasive regions were negative in all four type C tumors with p16 HDs. This result strongly supports the reliability of MLPA analysis for the detection of p16 HDs in primary lung adenocarcinomas. Thus, it was concluded that p16 protein is not expressed in a considerable fraction of small-sized lung adenocarcinomas due to HDs of the p16 gene. The consistency of the results of immunohistochemistry with that of MLPA analysis further supports the hypothesis that *p16* HD occurs early in lung adenocarcinoma progression.

Previously, Dr. Noguchi, who is one of the authors of this article, and his colleagues reported that 29 of 57 (51%) small-sized lung adenocarcinomas of types A to F were negative for p16 immunostaining (7). In their report, the frequency of p16 negativity was higher in smokers and in patients with non-BACs. Aberrant methylation of the *p16* gene promoter was detected more frequently in advanced BACs (type C) and non-BAC (types D–F) than in BACs (types A and B). In this study, the overall frequency (54%) of p16 negativity was quite similar to their reports, and the frequency was also higher in smokers than in nonsmokers (9 of 13 versus 6 of 15), and in type D (5 of 5) than in type B (7 of 15) or type C (3 of 8). Thus, it was highly suggested that a majority of cases with negative p16 expression without p16 HDs could be due to methylation of the *p16* gene promoter and the methylation was associated with tobacco smoking. However, methylation and HD are not likely to coexist with each other because the regions of HDs in most of the 13 cases with HDs included the promoter region of the *p16* gene (from probe no. 8 to probe no. 11). Thus, either methylation or HD of the *p16* gene was suggested to occur equally and independently in smokers, whereas HD dominates in nonsmokers.

Association of p16 HDs with clinicopathologic characteristics. We then investigated the association of p16 HDs with clinicopathologic characteristics, including smoking history, of